

# Covariation between oxygen and hydrogen stable isotopes declines along the path from xylem water to wood cellulose across an aridity gradient

Meisha Holloway-Phillips<sup>1,2</sup> , Lucas A. Cernusak<sup>3</sup> , Daniel B. Nelson<sup>1</sup> , Marco M. Lehmann<sup>2</sup> ,  
Guillaume Tcherkez<sup>4,5</sup>  and Ansgar Kahmen<sup>1</sup> 

<sup>1</sup>Department of Environmental Sciences-Botany, University of Basel, 4056, Basel, Switzerland; <sup>2</sup>Research Unit of Forest Dynamics, Research Group of Ecosystem Ecology, Stable Isotope Research Centre, Swiss Federal Institute for Forest, Snow and Landscape Research WSL, 8903, Birmensdorf, Switzerland; <sup>3</sup>College of Science and Engineering, James Cook University, Cairns, Qld, 4878, Australia; <sup>4</sup>Research School of Biology, College of Science, Australian National University, Canberra, ACT, 2601, Australia; <sup>5</sup>Institut de Recherche en Horticulture et Semences, Université d'Angers, INRAe, 42 rue Georges Morel, 49070, Beaucauzé, France

## Summary

Author for correspondence:  
Meisha Holloway-Phillips  
Email: [meisha.holloway@wsl.ch](mailto:meisha.holloway@wsl.ch)

Received: 17 January 2023  
Accepted: 16 August 2023

New Phytologist (2023)  
doi: 10.1111/nph.19248

**Key words:** aridity, Australia, cellulose, hydrogen isotopes, isotope tree-ring, oxygen isotopes, paleo-environmental reconstruction.

- Oxygen and hydrogen isotopes of cellulose in plant biology are commonly used to infer environmental conditions, often from time series measurements of tree rings. However, the covariation (or the lack thereof) between  $\delta^{18}\text{O}$  and  $\delta^2\text{H}$  in plant cellulose is still poorly understood.
- We compared plant water, and leaf and branch cellulose from dominant tree species across an aridity gradient in Northern Australia, to examine how  $\delta^{18}\text{O}$  and  $\delta^2\text{H}$  relate to each other and to mean annual precipitation (MAP).
- We identified a decline in covariation from xylem to leaf water, and onwards from leaf to branch wood cellulose. Covariation in leaf water isotopic enrichment ( $\Delta$ ) was partially preserved in leaf cellulose but not branch wood cellulose. Furthermore, whilst  $\delta^2\text{H}$  was well-correlated between leaf and branch, there was an offset in  $\delta^{18}\text{O}$  between organs that increased with decreasing MAP.
- Our findings strongly suggest that postphotosynthetic isotope exchange with water is more apparent for oxygen isotopes, whereas variable kinetic and nonequilibrium isotope effects add complexity to interpreting metabolic-induced  $\delta^2\text{H}$  patterns. Varying oxygen isotope exchange in wood and leaf cellulose must be accounted for when  $\delta^{18}\text{O}$  is used to reconstruct climatic scenarios. Conversely, comparing  $\delta^2\text{H}$  and  $\delta^{18}\text{O}$  patterns may reveal environmentally induced shifts in metabolism.

## Introduction

The potential for hydrogen (H) and oxygen (O) isotope analysis of plant cellulose to yield inferences about past climates and physiological processes has long been recognised (Schiegl & Vogel, 1970; Epstein *et al.*, 1976; Gray & Thompson, 1976; Libby *et al.*, 1976). However, despite its research history, substantial uncertainty remains around the exact biological and environmental information recorded in cellulose, limiting its application to tree-ring archives (e.g. Yakir, 1992; McCarroll & Loader, 2004; Gessler *et al.*, 2014).

The source of all organically bound hydrogen and the majority of oxygen in organic molecules derives from plant water. Compared with root and xylem stem water (i.e. 'source' water), leaf water becomes enriched in the heavier isotopes ( $^{18}\text{O}$  and  $^2\text{H}$ ) during transpiration (Dongmann *et al.*, 1974; Leaney *et al.*, 1985; Flanagan *et al.*, 1991; Farquhar & Lloyd, 1993).

The climatic and physiological processes that influence the isotopic composition of leaf water are well-understood and lead to predictable relationships between oxygen and hydrogen isotope compositions ( $\delta$ ) of leaf water (Cernusak *et al.*, 2016, 2022). As primary sugars are synthesised in leaves, sugars and by extension plant cellulose should theoretically show similar  $\delta^{18}\text{O}$ – $\delta^2\text{H}$  covariation as plant water due to the incorporation of O and H sourced both directly and indirectly from water during compound biosynthesis. Across large spatial scales, this appears to be a reasonable assumption (Lehmann *et al.*, 2022). However, at the local scale, analysing temporal variation in tree-ring chronologies, weak relationships between  $\delta^2\text{H}$  and  $\delta^{18}\text{O}$  are often observed (Nabeshima *et al.*, 2018; Nakatsuka *et al.*, 2020; Vitali *et al.*, 2022). This perhaps explains why the climate sensitivity of one element is often found to be different to the other (e.g. Loader *et al.*, 2008; Boettger *et al.*, 2014; Gori *et al.*, 2015) – although not always (e.g. Hafner *et al.*, 2011; An *et al.*, 2014).

Oxygen and hydrogen cellulose isotope models provide a useful framework to understand the drivers of isotopic variation (Yakir & DeNiro, 1990; Barbour & Farquhar, 2000; Roden *et al.*, 2000). They are conceptualised as a two-pool mixing model reflecting the initial synthesis of sugars via photosynthesis in source tissue (i.e. leaves) and its subsequent export to sink tissue (e.g. developing leaves, wood) where some isotope exchange with sink cell water can occur during sugar metabolism. Most applications have assumed that biochemical isotope effects in the models are invariant. However, recent studies have challenged this assumption. For example, the incorporation and exchange of oxygen from water in organic matter, which is an equilibrium isotope process, is thought to vary with temperature (Sternberg & Ellsworth, 2011), and the extent to which isotopic exchange occurs with water during sink cell metabolism has been shown to exhibit considerable variation, particularly in response to the environment (reviewed in Song *et al.*, 2022).

Initial estimates of hydrogen isotope effects during carbohydrate biosynthesis suggested that there is a large isotope fractionation against  $^2\text{H}$  during the Calvin–Benson–Bassham cycle ( $-171\%$ ), whereas the sum of hydrogen isotope fractionation during postphotosynthetic isotope exchange and metabolism is in favour of  $^2\text{H}$  ( $+158\%$ ) (Yakir & DeNiro, 1990). However, the constancy of these values has also been challenged on both theoretical (Cormier *et al.*, 2018; Zhou *et al.*, 2018) and experimental (Holloway-Phillips *et al.*, 2022; Schuler *et al.*, 2023) grounds. Also, position-specific intramolecular  $\delta^2\text{H}$  analysis has suggested different fractionation factors for individual H-atom positions, which respond to environmental conditions (Schleucher *et al.*, 1999; Augusti *et al.*, 2006; Wieloch *et al.*, 2022a,b). Variation in the isotopic offset between cellulose  $\delta^2\text{H}$  and plant water pools also supports the view that fractionation factors can change with species and growth conditions (Sternberg & Deniro, 1983; Cormier *et al.*, 2018, 2019; Baan *et al.*, 2022, 2023; Lehmann *et al.*, 2022).

As long as the extent to which sink cell isotopic exchange occurs and the values for biosynthetic fractionation remain constant or change proportionally between elements, covariation between  $\delta^{18}\text{O}$  and  $\delta^2\text{H}$  will persist through biosynthetic transformations from source water to cellulose. However, there are several reasons to explain a potential decoupling between  $\delta^{18}\text{O}$  and  $\delta^2\text{H}$  values:

(1) First, using the default model parameterisation of the cellulose isotope models and assuming normal leaf and xylem water isotope patterns observed in nature, the cellulose isotope models predict that whilst variation in xylem and leaf water  $\delta$  values result in positive covariation, variation in the fraction of sugars that undergo isotopic exchange in sink cells ( $f$ ) results in negative covariation (when all other variables are held constant). This is because an increase in  $f$  lowers cellulose  $\delta^{18}\text{O}$  values (greater proportion of sugars derived from an  $^{18}\text{O}$ -depleted xylem water pool compared to leaf water), and increases  $\delta^2\text{H}$  values (in this case, the large positive isotope fractionation during heterotrophic sugar metabolism outweighs the  $^2\text{H}$ -depleted xylem water pool as  $f$  increases). Thus, where cellulose isotopic variation is driven by variability in both plant water and  $f$ , the

relationship between  $\delta^{18}\text{O}$  and  $\delta^2\text{H}$  has the potential to weaken and/or invert.

(2) Second, variability in isotope fractionation during compound biosynthesis would add another mechanism by which the  $\delta^{18}\text{O}$ – $\delta^2\text{H}$  covariation may disappear, especially given that hydrogen is subject to additional kinetic isotope effects (during enzymatic reactions) that do not impact oxygen (discussed in Holloway-Phillips *et al.*, 2022 and elaborated on in the Discussion section).

(3) Third, tissue-specific patterns have been observed for both cellulose  $\delta^{18}\text{O}$  (Cheesman & Cernusak, 2016) and  $\delta^2\text{H}$  (Ish-Shalom-Gordon *et al.*, 1992; Ruppenthal *et al.*, 2015; Sanchez-Bragado *et al.*, 2019), suggesting that different C sources and metabolism in sink and source tissues can influence the extent to which climatic  $\delta^{18}\text{O}$  and  $\delta^2\text{H}$  signals are recorded by plant cellulose (Barnard *et al.*, 2007; Offermann *et al.*, 2011; Gessler *et al.*, 2013; Kimak *et al.*, 2015; Zhu *et al.*, 2020; Lehmann *et al.*, 2021).

However, there is a lack of studies that have tested whether noncovariation in  $\delta^{18}\text{O}$ – $\delta^2\text{H}$  is driven by variable biochemical isotope effects in one or both elements, and whether this depends on the tissue type assessed and plant compounds analysed (lipids, cellulose, lignin). For example,  $\delta^{18}\text{O}$  in wood cellulose from eucalypts across a climatic gradient in north-eastern Australia showed no climatic trend (Cheesman & Cernusak, 2016). By contrast,  $\delta^2\text{H}$  in leaf wax *n*-alkanes across another similar Australian transect recorded the leaf-water climatic signal, suggesting that the biochemical isotope effects were invariant with environmental conditions (Kahmen *et al.*, 2013).

To clarify the origin of the potential decoupling between  $\delta^{18}\text{O}$  and  $\delta^2\text{H}$  in organic compounds, we examined both  $\delta^{18}\text{O}$  and  $\delta^2\text{H}$  in leaf and branch-wood cellulose from dominant tree species, including eucalypts and acacia, sampled across a 1500-km climatic gradient in northern Australia (Hutley *et al.*, 2011), where leaf water enrichment was largely driven by both site variation in relative humidity (RH) and RH-independent changes in the isotope composition of xylem water (Kahmen *et al.*, 2013; Cernusak *et al.*, 2016). We addressed the following questions: (1) Is there a  $\delta^{18}\text{O}$ – $\delta^2\text{H}$  decoupling in cellulose, and if so, is the loss of the climatic isotope signal element dependent? (2) Can we see differences in the delta values between organs and if so, does it relate to expected differences in biochemistry? We then used cellulose isotope models parameterised with commonly accepted values and looked at whether the discrepancy between modelled estimates and observed  $\delta^{18}\text{O}$  and  $\delta^2\text{H}$  values of leaf and branch wood cellulose followed an aridity-dependent isotopic offset in order to suggest predictable shifts in biochemical isotope effects.

## Materials and Methods

### Field sites, species, and sampling of plant material

We made use of leaf and wood (branch) xylem samples collected within the original sampling campaign published in part by Kahmen *et al.* (2013). The study sampled 11 sites spanning 1500 km from Alice Springs to Darwin in the Northern Territory,

Australia, as part of the North Australian Tropical Transect (Hutley *et al.*, 2011; Fig. 1). For the study of Kahmen *et al.* (2013), only six of the 11 sites were analysed for the  $\delta^2\text{H}$  of *n*-alkanes in leaf waxes. The isotopic composition of leaf water was also sampled diurnally (four time points) at five of the 11 sites, and the data set published in full by Cernusak *et al.* (2016). Across all sites, branch xylem was collected for water extraction, and subsequently used for cellulose isotope analyses. Branch sections were *c.* 1 cm diameter, that is 'twigs'. Leaf tissue was also collected at all 11 sites and similarly used for cellulose isotope analyses. Until this study, the cellulose isotope information had not been published. For further details on when the samples were collected and processed, see Supporting Information Dataset S1 – 'Metadata'.

Across the sites, long-term mean annual precipitation (MAP) and mean relative humidity (RH) ranged from 313 mm yr<sup>-1</sup> and 34% in Alice Springs to 1739 mm yr<sup>-1</sup> and 62% in Darwin. Mean annual temperature across sites was much less variable (see Dataset S1 – 'Metadata' for source information). The two dominant genera, represented across most sites, were *Acacia* and *Eucalyptus*, as well as the genus *Corymbia*, which is phylogenetically close to *Eucalyptus* (see Dataset S1 – 'Isotopic data' for information on which species were represented at each site).

At each site, five to six mature trees of a single acacia or eucalypt species were sampled for leaf and branch material in April 2010 at the end of the wet season. Samples were randomly collected from the sunlit canopy of trees, and bulked, respectively, per replicate tree. Whole leaves were placed in paper bags and the bark of branch material was immediately removed, and the samples sealed in Exetainer<sup>®</sup> vials (Labco Ltd, Lampeter, UK). All material was kept on ice during transportation before being dried in paper bags at 60°C for 48 h in a drying oven. In the case of the branch material, xylem water was first extracted before being oven-dried.

## Cellulose purification

After drying, leaves and wood were ground to a fine powder using a ball mill (Retsch, Düsseldorf, Germany), before cellulose was purified according to the method of Gaudinski *et al.* (2005). Briefly, *c.* 200 mg of ground material was sealed into Ankom bags. The lipids were extracted by reflux in a Soxhlet apparatus with 2 : 1 toluene : ethanol (95%) mixture for *c.* 24 h under high heat, and then under ethanol only until the solvent was clear. Samples were air-dried before being boiled in deionised water for 4 h to remove water-soluble sugars. Lignin was removed with a bleaching solution of sodium chlorite and acetic acid (pH 4) under ultrasonic bath at 70°C for *c.* 24 h. Finally,  $\alpha$ -cellulose was purified from holocellulose with a 15% sodium hydroxide solution at room temperature in an ultrasonic bath. Samples were oven-dried at 50°C for 3 d before being rehomogenised in 2.0-ml tubes.

## Isotope analysis

Cellulose was analysed for  $\delta^{18}\text{O}$  and  $\delta^2\text{H}$  according to Holloway-Phillips *et al.* (2022) in the Stable Isotope Ecology Lab at the University of Basel. Long-term analytical precision for  $\delta^{18}\text{O}$  was monitored through repeated analysis of additional quality control samples and was 0.24‰ ( $n = 188$ ) for samples analysed in 2018. An online dual-equilibration technique was used for analysis of the nonexchangeable hydrogen  $\delta^2\text{H}$  (Wassenaar *et al.*, 2015). This method aims to account for the exchangeable hydrogen on hydroxy groups by exchanging with hydrogen from water vapour of known  $\delta^2\text{H}$  value. The fraction of exchangeable hydroxy hydrogen relative to total hydrogen, expressed as  $X_e$ , is in theory 30% for cellulose (Schuler *et al.*, 2022). We observed values of *c.* 6%, suggesting that we did

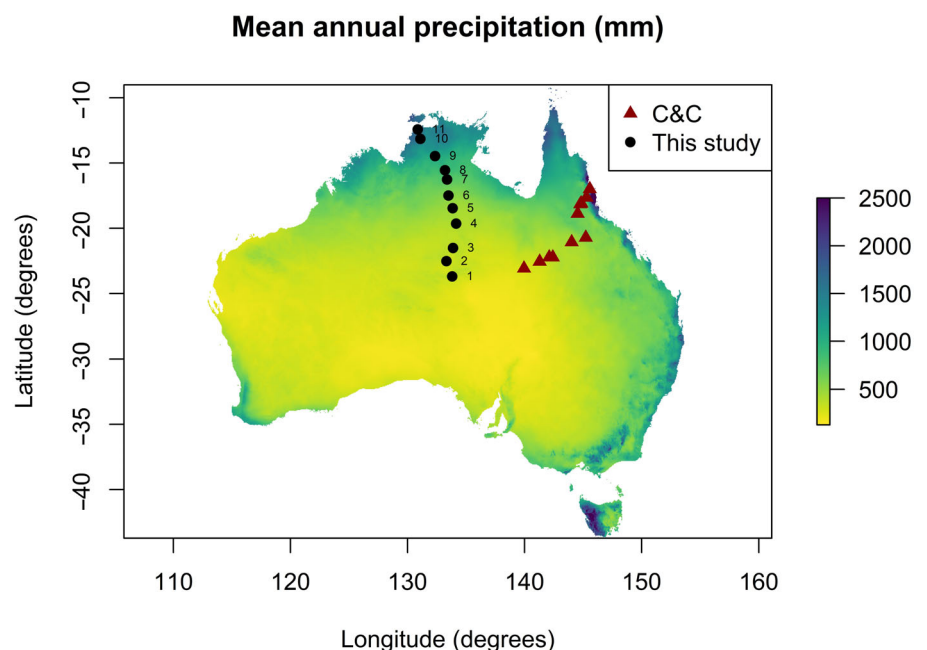


**Fig. 1** Map of Australia showing spatial distribution of long-term mean annual precipitation (1976–2005) at 0.01° resolution (Hutchinson *et al.*, 2014), with site locations for the North Australian Tropical Transect (Hutley *et al.*, 2001) ('This study'), and the comparative aridity gradient of Cheesman & Cernusak (2016) ('C&C').

not equilibrate all hydrogen on hydroxy groups; but this is similar to the theoretical fraction of freely exchangeable hydroxy hydrogen under normal conditions (Meier-Augenstein *et al.*, 2014). That said, to determine whether the low  $X_c$  values caused systematic bias in our data set, we analysed a subset of leaf and branch wood samples by the same method as Schuler *et al.* (2022), at the Swiss Federal Institute for Forest, Snow and Landscape Research (WSL), where higher  $X_c$  values were obtained. We found a very strong correlation between the two methods (leaf tissue,  $R^2 = 0.92$  and branch wood tissue;  $R^2 = 0.97$ ; Fig. S1). Despite there being a small statistically significant offset between the two methods (intercept  $-14.92\text{‰}$  and  $-7.10\text{‰}$  for leaf and branch wood, respectively) and a small statistically significant deviation of the slope from 1 (slope 1.05 and 1.14 for leaf and branch wood, respectively), the slopes of  $\delta^2\text{H}$  and  $\delta^{18}\text{O}$  between analytical methods for each tissue were not significantly different from each other suggesting that inferences made between elements are robust (data not shown). This was confirmed with a sensitivity analysis (Notes S1). Thus, we chose to present the original data where we had good confidence on the internal consistency of the analyses. Analytical performance of the dual-water exchange method at the University of Basel was monitored through routine analysis of bulk cellulose (Sigma-Aldrich) and an in-house quality control standard consisting of powdered *Fagus* leaves. The  $\delta^2\text{H}$  values of the nonexchangeable hydrogen in these materials were  $-50.7 \pm 1.3\text{‰}$  ( $n = 242$ ) and  $-66.0 \pm 1.6\text{‰}$  ( $n = 224$ ), respectively, during the year over which analyses were conducted.

Isotopic values are reported either as isotopic compositions ( $\delta$ ), defined as:

$$\delta_{\text{sample}} = \frac{R_{\text{sample}}}{R_{\text{std}}} - 1 \quad \text{Eqn 1}$$

where,  $R_{\text{sample}}$  is the isotope ratio of the measured sample and  $R_{\text{std}}$  is the isotope ratio of VSMOW, or as enrichment above source (xylem) water ( $\Delta$ ), which was calculated as:

$$\Delta_{\text{compound}} = \frac{\delta_{\text{compound}} - \delta_{\text{XW}}}{1 + \delta_{\text{XW}}} \quad \text{Eqn 2}$$

where,  $\delta_{\text{XW}}$  is the isotopic composition of xylem water and  $\delta_{\text{compound}}$  refers to the compound measured. Isotopic values were multiplied by 1000 to scale to per mil (‰). Isotopic enrichment above source water is particularly useful to isolate the impact of leaf water evaporative enrichment and the extent to which this signal is transferred to cellulose.

### Modelling cellulose isotopic composition: theory and parameters

The seasonally integrated isotope composition of leaf and branch cellulose ( $\delta_{\text{cellulose}}$ ) can be modelled according to a generalised two-process model: one fraction ( $1 - f$ ) of O and carbon-bound H comes from leaf water ( $\delta_{\text{LW}}$ ) during photosynthetic reactions

with biosynthetic fractionation,  $\epsilon_A$ . The other fraction ( $f$ ) comes from water in developing cells ( $\delta_{\text{sink\_water}}$ ) during postphotosynthetic reactions in developing leaves or stem cambium, with biosynthetic fractionation,  $\epsilon_H$  (Yakir & DeNiro, 1990; Roden *et al.*, 2000; Holloway-Phillips *et al.*, 2022):

$$\delta_{\text{cellulose}} = (1-f)(\delta_{\text{LW}}(1 + \epsilon_A) + \epsilon_A) + f(\delta_{\text{sink\_water}}(1 + \epsilon_H) + \epsilon_H) \quad \text{Eqn 3}$$

The isotope composition of bulk leaf water is generally less enriched in the heavier isotope compared with the estimated isotope composition of water at evaporative sites ( $\delta_e$ ) (Cernusak *et al.*, 2016). However, in Kahmen *et al.*'s (2013) study, diurnal observations of  $\delta_{\text{LW}}$  were well-predicted by the Craig-Gordon equation for leaf evaporative sites (Fig. S2),  $\delta_e$  (Farquhar & Lloyd, 1993; Cernusak *et al.*, 2016) and there was no evidence of a Péclet effect (Fig. S3). Furthermore, a sensitivity analysis using an empirical correction between the observed diurnally measured values and the Craig-Gordon leaf water estimates, indicated that it did not change the interpretation of the data (Notes S1). Therefore, we also used the Craig-Gordon equation here to estimate seasonally averaged  $\delta_{\text{LW}}$  for both elements:

$$\delta_e = (1 + \epsilon^+) \left( (1 + \epsilon_k)(1 + \delta_E) \left( 1 - \frac{e_a}{e_i} \right) + \frac{e_a}{e_i} (1 + \delta_v) \right) - 1 \quad \text{Eqn 4}$$

where  $\epsilon^+$  is the isotope fractionation between liquid water and vapour at equilibrium,  $\epsilon_k$  is the fractionation during diffusion of water from the leaf intercellular airspaces to the atmosphere,  $\delta_E$  is the isotope composition of transpired vapour, which at steady-state is equal to xylem water ( $\delta_{\text{XW}}$ ),  $e_a/e_i$  is the ratio of ambient to intercellular saturated vapour pressure, and  $\delta_v$  is the isotope composition of atmospheric water vapour.

Enriched water from the leaf mesophyll can be transferred to developing cells by translocation in the phloem. As such,  $\delta_{\text{sink\_water}}$  can be modelled as a mixture of xylem ( $\delta_{\text{XW}}$ ) and leaf water, where the proportion of unenriched xylem water is often termed  $p_X$ . For simplicity, we assumed that  $p_X = 1$ , that is  $\delta_{\text{sink\_water}} = \delta_{\text{XW}}$ , which is a good assumption for wood, but for leaves, it may be the case that  $p_X < 1$  (Cernusak *et al.*, 2005; Liu *et al.*, 2017).

For modelling the  $\delta^{18}\text{O}$  value in cellulose,  $f_O$  (also referred to as  $p_{\text{ex}}$  in the literature) is assumed to be *c.* 0.4 (Song *et al.*, 2022). We use 0.39 based on studies that also measured  $f_H$  (Table S1). Isotope fractionation between carbonyl-O and water ( $\epsilon_A$  and  $\epsilon_H$  in Eqn 3) is denoted as  $\epsilon_{\text{wc}}$  and taken to be the same value for photosynthetic and postphotosynthetic reactions. The value of  $\epsilon_{\text{wc}}$  is *c.* 27‰ (Cernusak *et al.*, 2003), which we corrected for temperature using the empirical relationship in Sternberg & Ellsworth (2011). For modelling the  $\delta^2\text{H}$  value in cellulose, we used the commonly applied parameter values for  $\epsilon_A = -171\text{‰}$  and  $\epsilon_H = +158\text{‰}$  (Yakir & DeNiro, 1990; Roden *et al.*, 2000), and the average literature value of  $f_H$  of  $0.38 \pm 0.06$  (Table S1).



## Assumptions to integrate the cellulose isotope signature on a seasonal basis

To estimate seasonally integrated cellulose isotope values, long-term mean annual 09:00 and 15:00 h observations of RH and air temperature ( $T_{\text{air}}$ ) were obtained from the Australian Bureau of Meteorology ([www.bom.gov.au](http://www.bom.gov.au)) (see Dataset S1 for more detail on weather station number and data collection date range for each station). As it is not known how variable the phenological patterns were across sites, we took the pragmatic approach of using annually averaged information to represent gross differences in site climate. This approximation is reasonable provided we do not seek to estimate exact values, but instead aim to replicate any patterns associated with changes in site climatic conditions along the spatial gradient. This is further justified because leaves were chosen randomly and thus represent an annual cohort of leaves. In addition, wood growth, whilst peaking at certain times of the year, can utilise both carbon reserves stored at different times of the year and current assimilates. The isotope composition of water vapour was measured along with leaf water during the diurnal campaigns. However, as the day of sampling is not necessarily representative of longer term water vapour isotopic patterns, we assumed that the water vapour is in isotopic equilibrium with the measured xylem water, which was sampled in March and September 2010, and which integrates the meteoric water isotope signals over longer timescales (see Kahmen *et al.*, 2013 for more details). The kinetic isotope fractionation for the leaf water model,  $\epsilon_k$ , was calculated using the average of all stomatal conductance observations (Cernusak *et al.*, 2016). Note that the calculation of  $\delta_{\text{LW}}$  is fairly insensitive to uncertainty in stomatal conductance (e.g.  $\pm 0.2 \text{ mol m}^{-2} \text{ s}^{-1}$  equates to less than  $\pm 0.04\%$  for oxygen and  $\pm 0.06\%$  for hydrogen). For a summary of the model inputs and data sources, see Table S2.

## Derived model parameters

There are up to four parameters in the cellulose isotope model that could theoretically vary:  $f$ ,  $\epsilon_A$ ,  $\epsilon_H$  and  $\delta_{\text{sink\_water}}$  as a function of  $p_x$  (Eqn 3); but, to model the isotopic composition of cellulose, a value for each parameter must be assumed. However, if the isotope composition of cellulose is known, any discrepancy between modelled and measured isotopic compositions of cellulose can be removed by adjusting the value of one of the model parameters, that is parameter estimation via model inversion. At this stage, hydrogen and oxygen must be considered separately.

For oxygen, the discrepancy between modelled and observed  $\delta_{\text{cellulose}}$  has previously been explained according to either variation in  $f_O$ , assuming  $T_{\text{leaf}} = T_{\text{air}}$  (e.g. Cheesman & Cernusak, 2016), or decoupling between leaf and air temperature, assuming  $f_O$  is constant (e.g. Helliker & Richter, 2008; Song *et al.*, 2011). As Kahmen *et al.* (2013) observed minimal difference between leaf and air temperature during diurnal measurements, we do not consider leaf temperature decoupling to be an issue in this study. An empirical relationship developed using Australian published observations of leaf and air temperature

(229 observations) also indicated close agreement (McInerney *et al.*, 2023), which is the relationship we adopted in this study to estimate seasonally integrated leaf temperature for modelling the leaf water isotopic composition (Eqn 4). Similarly, variability in  $\epsilon_{\text{wc}}$  is assumed to only vary as a function of temperature, which we accounted for. Thus, rationalising the observed  $\delta_{\text{cellulose}}$  values by solving for  $f_O$  seems justified, especially for wood where  $p_x = 1$  is a good assumption. Eqn 3 can thus be rearranged to solve for  $f_O$ :

$$f_O = \frac{\delta_{\text{cellulose}} - \delta_{\text{LW}}(1 + \epsilon_{\text{wc}}) - \epsilon_{\text{wc}}}{(\delta_{\text{xylem}} - \delta_{\text{LW}})(1 + \epsilon_{\text{wc}})} \quad \text{Eqn 5}$$

For hydrogen, there is evidence that all biochemical parameters ( $f$ ,  $\epsilon_A$ ,  $\epsilon_H$ ) could vary, and on a mathematical basis, there is negative compensation between parameters (Holloway-Phillips *et al.*, 2022). Thus, rather than arbitrarily choosing a variable to rationalise the discrepancy between observed and modelled  $\delta_{\text{cellulose}}$  values for hydrogen, we instead asked the more general question of whether any modelled discrepancy related to site aridity, so that a model correction could be used across similar environmental gradients. For this purpose, we take mean annual precipitation as representative of site aridity (Hutley *et al.*, 2011; Nijzink & Schymanski, 2022), which is inversely related to aridity (taken as potential evapotranspiration/mean annual precipitation) to a close approximation (refer to Dataset S1 – ‘Metadata’).

## Data analysis

All statistical analyses were conducted in R (v.3.6.1, R Core Team, 2019) with RSTUDIO (v.1.2.1335, [www.rstudio.com](http://www.rstudio.com)). Fig. 1 was produced using packages NCDF4 (Pierce, 2023), RASTER (Hijmans, 2023), RGDAL (Bivand *et al.*, 2023), GGLOT2 (Wickham, 2016), RCOLORBREW (Neuwirth, 2022), PRISMATIC (Hvitfeldt, 2022) and VIRIDISLITE (Garnier *et al.*, 2022). Dual isotope plots (Fig. 2) and covariation between plant tissues (Fig. 3) were investigated using standard major axis regression due to large natural variation between individual trees, with the ‘sma’ function in the package SMATR (Warton *et al.*, 2012). Outliers were considered with the ‘robust = T’ option, which uses Huber’s  $M$  estimation in place of least squares. Relationships were modelled values were regressed against observations (Fig. 4), or the model discrepancy (defined as  $\epsilon_{\text{exp-obs}} = ((\delta_{\text{exp}} - \delta_{\text{obs}})/(1 + \delta_{\text{obs}}))$ ) and  $f_O$  estimates were regressed against mean annual precipitation (Figs 5, 6), were investigated using ordinary least squares regression with the ‘lm’ function in the base R package STATS. Separate analyses for each genus were not performed as acacia was not represented across all sites. Also, given species within a genus varied across sites, we had no *a priori* reason to suggest that species within a genus were more similar than between genera to warrant separating the two groups; that is, we did not have the power in this study to test the significance of species identity on isotope patterns. Figs 2–6 were graphed in SIGMAPLOT v.11 (SPSS Inc., Chicago, IL, USA).

To ensure that the interpretations of the model coefficients of Figs 4–6 were robust, we assessed alternative parameterisations

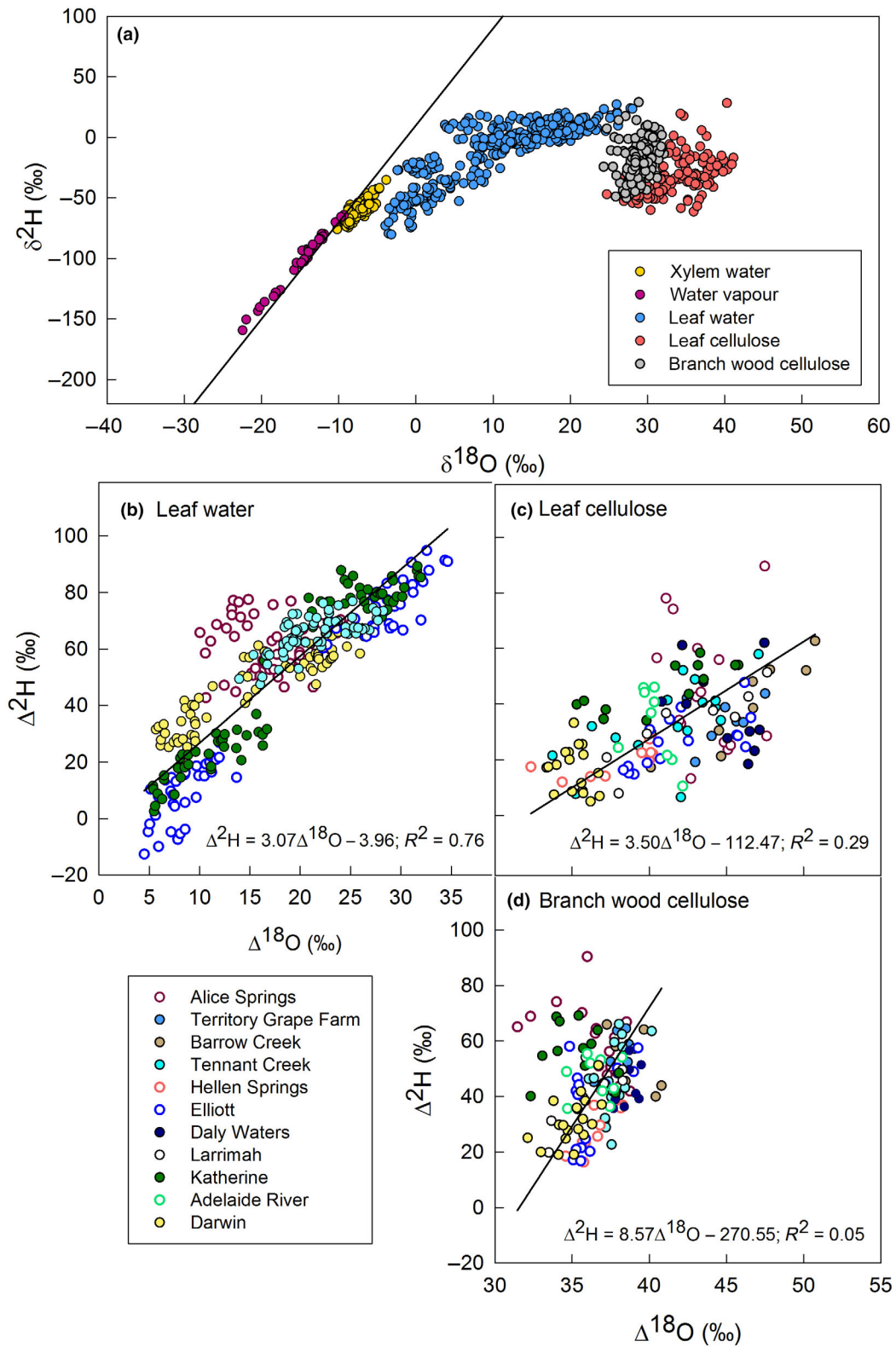


**Fig. 2** Observed covariation between hydrogen and oxygen isotopic compositions on a delta basis ( $\delta$ ) for xylem water, water vapour, leaf water, leaf cellulose and branch wood cellulose (a); and, on a  ${}^2\text{H}$ - ${}^{18}\text{O}$  enrichment basis ( $\Delta$ ) relative to xylem water, for leaf water (b), leaf cellulose (c) and branch wood cellulose (d). Data compiled from Cernusak *et al.* (2016) and this study. The solid line in (a) refers to the meteoric water line and in (b–d) reflect significant ( $P < 0.05$ ) regression lines fitted by standardised major axis regression.

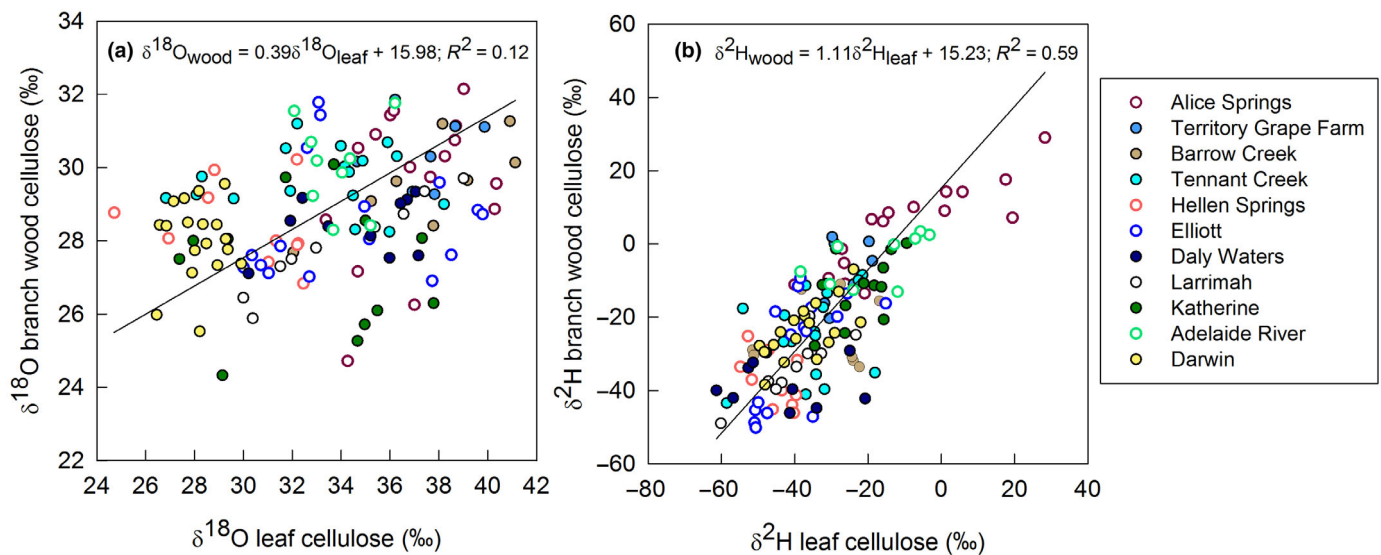


**Fig. 3** Observed covariation between branch wood and leaves for the oxygen isotope composition,  $\delta^{18}\text{O}$  (a) and hydrogen isotope composition,  $\delta^2\text{H}$  (b) of cellulose. Solid regression lines are significant ( $P < 0.05$ ) and fitted by standardised major axis regression. Slope and intercept significantly different from 1 and 0 for  $\delta^{18}\text{O}$ . For  $\delta^2\text{H}$ , the slope was not significantly different from 1, but intercept significantly different from 0. Colours represent different sites.

of the cellulose isotope model, which can be viewed in Notes S1 – Tables S3–S6. This included testing alternative assumptions for leaf temperature, the isotopic composition of water vapour, and the model used to estimate leaf water delta values, as well as the impact of the analytical method for the  $\delta^2\text{H}$  of leaf cellulose. As the sensitivity analysis indicated that there was minimal change to the conclusions, we only present the data based on the model parameterisations given in Table S2.

## Results

### $\delta^{18}\text{O}$ – $\delta^2\text{H}$ relationship in water and cellulose

Across the 1500 km aridity transect, the observed range in xylem water  $\delta$  values sampled from branches varied by 5‰ for  $\delta^{18}\text{O}$  and 35‰ for  $\delta^2\text{H}$  (Table 1). Both xylem and water vapour  $\delta$  values fell approximately on the global meteoric water line (GMWL; Fig. 2a; Table 2). Leaf water fell below the GMWL reflecting isotope fractionations during transpiration (Fig. 2a). Leaf cellulose had a similar slope to that of leaf water in the dual-isotope plot (3.47 vs 2.93; Table 2), but the  $\delta^{18}\text{O}$  values were all higher than those of leaf water  $\delta^{18}\text{O}$  values, whereas the  $\delta^2\text{H}$  values were within the range of the leaf water isotope  $\delta^2\text{H}$  values (Fig. 2a).

When isotope delta values were converted to enrichment above source water ( $\Delta$ ), leaf water and leaf cellulose also had similar slopes (Fig. 2b,c; slopes not significantly different), suggesting that the evaporative isotopic signal was partially retained within leaf cellulose (strength of the relationship *c.* 40% of that of leaf water covariation). We consider the comparison between leaf water and leaf and branch wood cellulose isotopic variation across sites (rather than within sites), given the different time-scales of integration (leaf water – diurnal; cellulose – seasonal). The slope of the regression between  $\Delta^2\text{H}$  vs  $\Delta^{18}\text{O}$  of branch wood cellulose (8.57) was much larger than that of leaf water

(3.07) (Fig. 2d vs Fig. 2b), and the  $\delta^2\text{H}/\delta^{18}\text{O}$  relationship had a similar slope as xylem water (although the relationship was weak,  $R^2 = 0.08$ , Table 2).

The change in slope between leaf and branch wood cellulose was largely driven by a compression in the  $\delta^{18}\text{O}$  range going from 16‰ (leaf cellulose) to 8‰ (wood cellulose), whilst the isotopic range was more conserved for  $\delta^2\text{H}$ : 90‰ (leaf cellulose) and 80‰ (wood cellulose) (Table 1). Consequently, there was little covariation between leaf and branch wood cellulose for  $\delta^{18}\text{O}$  ( $R^2 = 0.12$ ; Fig. 3a), but strong covariation for  $\delta^2\text{H}$  ( $R^2 = 0.59$ ; Fig. 3b). Notably, the strength of the correlation between  $\delta^2\text{H}$  and  $\delta^{18}\text{O}$  progressively weakened moving from plant water pools into cellulose: xylem water ( $R^2 = 0.83$ ) < leaf water ( $R^2 = 0.69$ ) < leaf cellulose ( $R^2 = 0.17$ ) < wood cellulose ( $R^2 = 0.08$ ) (Table 2). This pattern was also visible with isotope enrichments,  $\Delta$  (Fig. 2b–d).

### Comparison of observed and predicted isotope compositions

The majority of the variation in cellulose  $\delta^{18}\text{O}$ – $\delta^2\text{H}$  delta values could not be explained by the cellulose isotope models. In effect, modelled cellulose delta values assuming biochemical parameters are invariant, explained only 21% of leaf and 16% of branch wood cellulose  $\delta^{18}\text{O}$  values, and 19% of leaf and 35% of branch wood cellulose  $\delta^2\text{H}$  values (Fig. 4). There was a significant isotopic offset ( $\epsilon_{\text{exp-obs}}$ ) between modelled and observed leaf cellulose delta values for both leaf  $\delta^{18}\text{O}$  and  $\delta^2\text{H}$  (Fig. 5a,c). In contrast, for branch wood cellulose, there was a significant negative isotopic offset with mean annual precipitation (MAP), which explained 60% of the variation in the model discrepancy for the  $\delta^{18}\text{O}$  of branch wood cellulose (Fig. 5b). In comparison, only 3% of the model discrepancy in branch wood cellulose  $\delta^2\text{H}$  values could be explained by MAP (3%; Fig. 5d); in other words,

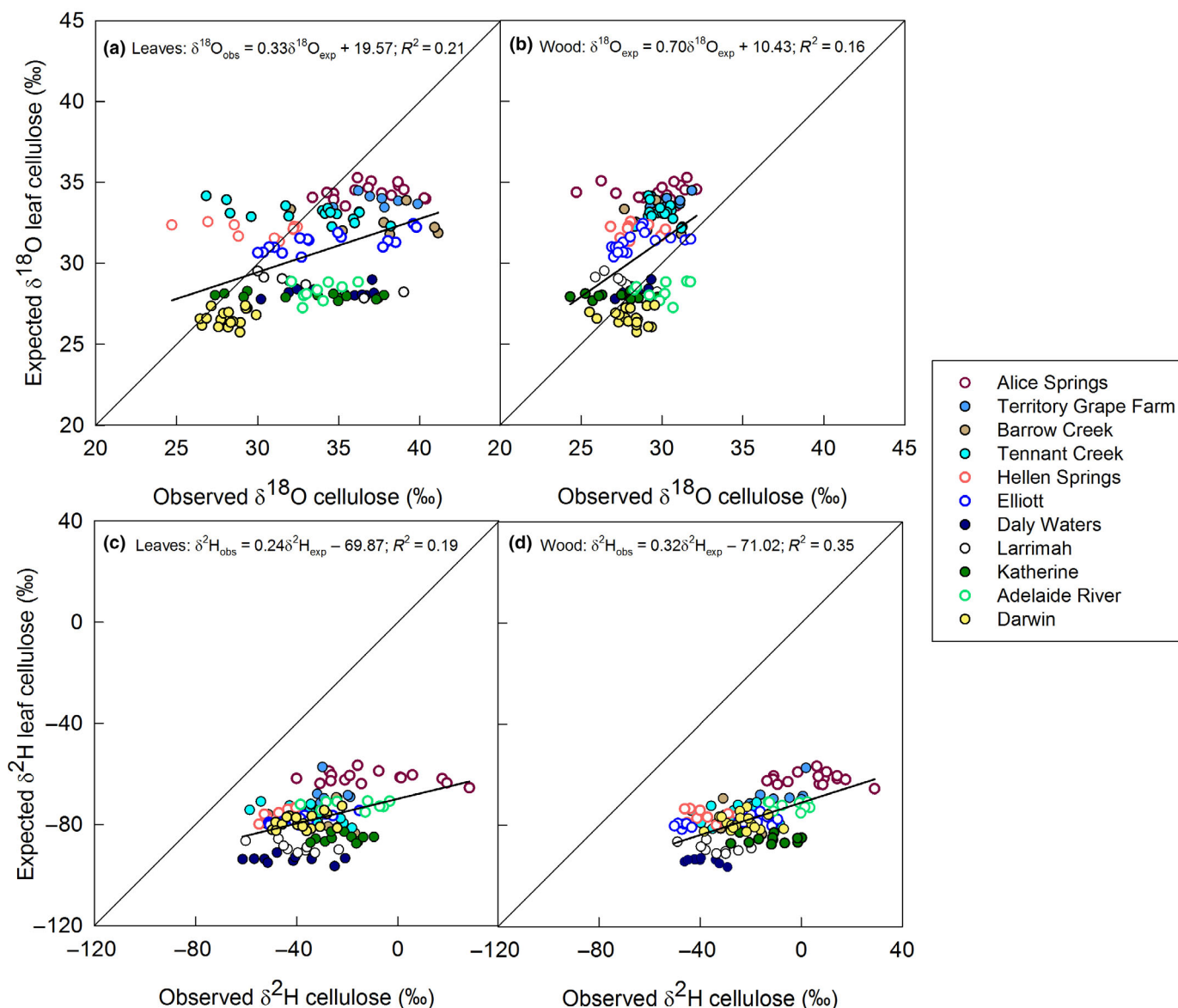


**Fig. 4** Relationship between expected and observed cellulose delta values for  $\delta^{18}\text{O}$  (a, b) and  $\delta^2\text{H}$  (c, d). Expected values were modelled according to Eqn 3, assuming biosynthetic isotope parameters are invariant (Supporting Information Table S2). Regression lines are significant ( $P < 0.05$ ) and fitted with ordinary least squares regression. 1 : 1 line also shown. Colours represent different sites.

biochemical parameters ( $f$ ,  $\epsilon_{\text{H}}$ , and  $\epsilon_{\text{A}}$ ) varied across sites independently of MAP.

Rationalising the discrepancy between modelled and observed values by varying the contribution of oxygen derived from xylem water ( $f_{\text{O}}$ ) is justified for oxygen since it is believed that changes in isotope fractionation ( $\epsilon_{\text{wc}}$ ) are minimal (see ‘Derived model parameters’ in the Materials and Methods section).  $f_{\text{O}}$  (calculated with Eqn 5 using temperature corrected  $\epsilon_{\text{wc}}$ ) in branch wood cellulose was always higher than that of leaf cellulose (Fig. 6a). With respect to mean annual precipitation, a negative correlation was found, which was particularly strong for branch wood cellulose. In fact,  $f_{\text{O}}$  decreased by 0.02 for every 100 mm increase in mean annual precipitation, compared with 0.01 for leaf cellulose (Fig. 6a). Interestingly, the relationship between  $f_{\text{O}}$  values associated with branch wood cellulose

and mean annual precipitation was not significantly different between this study and that obtained by Cheesman & Cernusak (2016) (Fig. 6b). However, the absolute values were found to be sensitive to the model parameterisation used (Fig. S4). For the interested reader, we provide (but do not interpret or discuss)  $f_{\text{H}}$  estimates, and alternatively rationalise the discrepancy according to  $p_{\text{x}}$ . A summary of site averaged  $f_{\text{O}}$ ,  $f_{\text{H}}$  and  $p_{\text{x}}$  values can be found in Table S7.

## Discussion

### $\delta^{18}\text{O}$ – $\delta^2\text{H}$ covariation depends on the plant organ

The extent to which climatic information is recorded by the  $\delta^{18}\text{O}$  and  $\delta^2\text{H}$  of plant cellulose has been mostly assessed in tree-



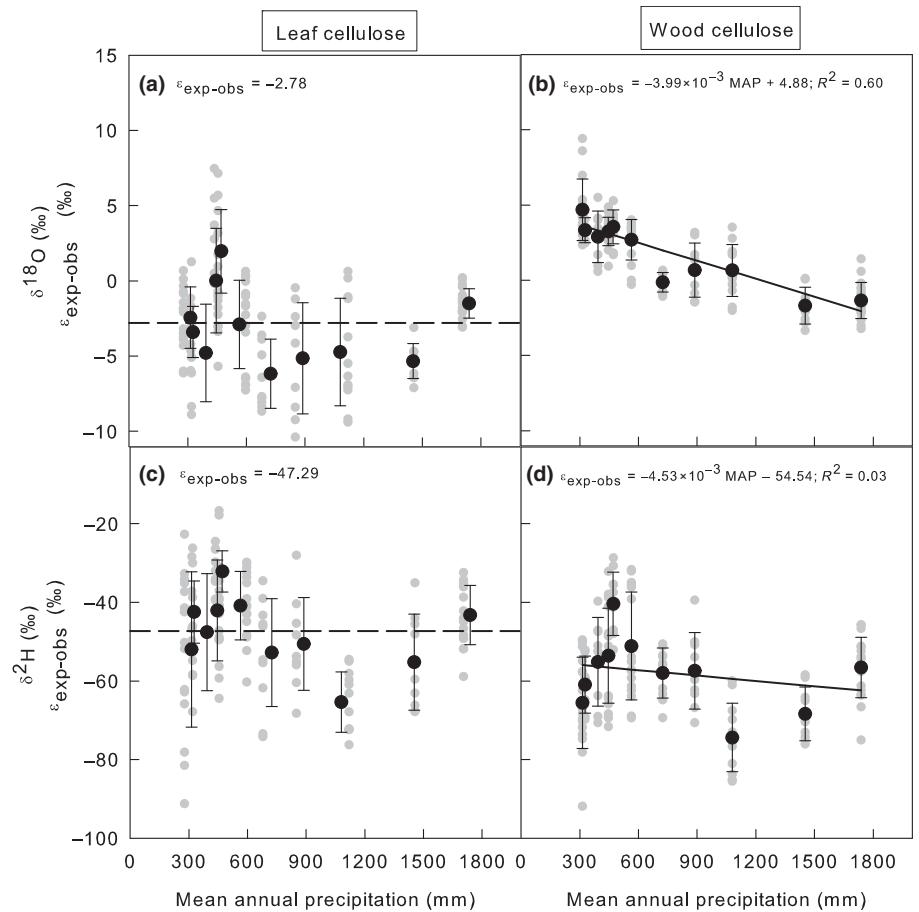


**Fig. 5** Isotopic offset ( $\epsilon_{\text{exp-obs}}$ ) between modelled and observed oxygen,  $\delta^{18}\text{O}$  (a, b) and hydrogen,  $\delta^2\text{H}$  (c, d) isotopic compositions ( $\delta$ ) as dependent on long-term mean annual precipitation, for leaf (a, c) or branch wood (b, d) cellulose. Individual plant values are shown by the grey circles; means are shown by the black circles with SD used for the error bars. Regression (solid) lines are significant ( $P < 0.05$ ) and fitted with ordinary least squares regression. Dashed lines indicate the intercept is significantly different from 0 ( $P < 0.05$ ).

rings where time provides the source of environmental variation. Using European-wide century-long timeseries, the climatic associations were found to be more consistent for O than for H, reflecting weak covariation between the two elements (Vitali *et al.*, 2022). Here, we also found that covariation was weakened in cellulose compared with plant water pools, despite the expected hydrologic isotope signals induced by the environmental gradient being larger in this study than is typically found within a timeseries of a given site. Moreover, covariation declined to a greater extent in branch wood cellulose compared with leaf cellulose (Fig. 2). Whilst the leaf water enrichment signal captured across the environmental gradient was partially retained within leaf cellulose  $\Delta$  values (Fig. 2c), the loss of covariation between  $\Delta^2\text{H}$  and  $\Delta^{18}\text{O}$  in branch wood cellulose (Fig. 2d) appeared to be driven by an aridity-dependent isotope effect that impacted oxygen but not hydrogen (Fig. 5). This is supported by the fact that the slope of the regression between leaf and wood cellulose  $\delta$  values was significantly different from unity for oxygen but not for hydrogen (Fig. 3). However,  $\delta^2\text{H}$  variation remained dominated by biochemical isotope effects based on the variability between expected and observed  $\delta$  values (Fig. 4c,d). The lack of simple (e.g. linear) environmental predictability to the modelled discrepancy (Fig. 5) adds increased complexity in accounting for biochemical-induced variation within cellulose isotope models. Below, we take advantage of the differential isotope patterns for oxygen and hydrogen between leaf and branch

wood cellulose to examine the biochemical origin of the  $\delta^{18}\text{O}$ – $\delta^2\text{H}$  decoupling.

### Principle of biochemistry impacting on $\delta^{18}\text{O}$ and $\delta^2\text{H}$

The main mechanism by which carbon metabolism has been hypothesised to enrich sugars in  $^2\text{H}$  and deplete in  $^{18}\text{O}$  in sink cells is isotopic exchange with source water, with corresponding equilibrium isotope effects. As highlighted by Holloway-Phillips *et al.* (2022), mechanisms for oxygen and carbon-bound hydrogen isotope exchange with solvent water are rather different, despite the reactions associated with isotope exchange being similar between the two elements (see Fig. S5 for a simplified schematic of the reactions involved). On the one hand, oxygen exchange with water occurs in carbonyl groups of sugars. This can occur during hydrolysis (e.g. aldolase reaction) or spontaneously, that is without a reaction needing to proceed (e.g. in carbonyl O of triose-phosphates), but the probability of exchange likely increases during enzymatic reactions that facilitate covalent bond breakage (e.g. reactions involving triosephosphate isomerase; TPI, and phosphoglucose isomerase; PGI) (Farquhar *et al.*, 1998). Based on studies that have compared the isotopic composition of leaf sucrose from terrestrial plants (Cernusak *et al.*, 2003), or cellulose of aquatic plants with isotopic measures of the leaf water pool or growth media (DeNiro & Epstein, 1981), respectively, isotopic equilibrium seems to be

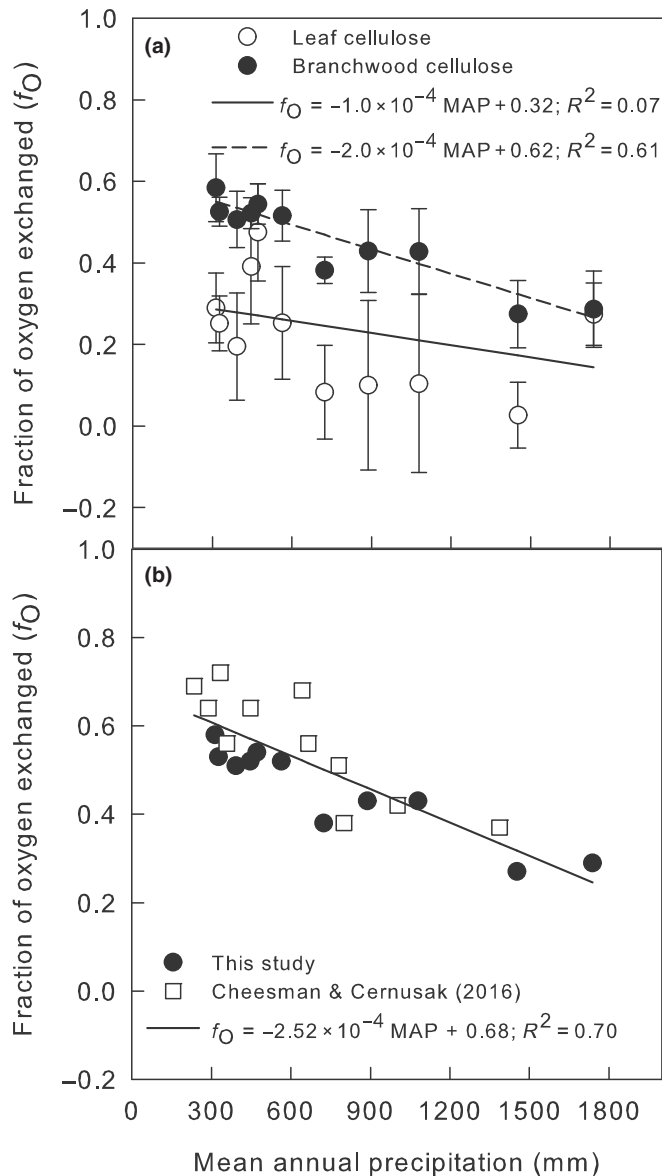


**Fig. 6** Relationship between the fraction of oxygen exchanged during sugar processing in sink cells ( $f_O$ ) with respect to long-term mean annual precipitation in leaf and branch wood cellulose (a) and with wood cellulose between studies (b). Note in (b), for this study values include those of both acacia and eucalypts combined, whereas the values of Cheesman & Cernusak (2016) relate only to eucalypt species. Mean values are shown in (a) with SD used for the error bars. Regression lines are significant ( $P < 0.05$ ) and fitted with ordinary least squares regression.

mostly achieved at the whole compound level for oxygen (Waterhouse *et al.*, 2013). On the other hand, exchange of C-bound hydrogen atoms with water always requires the facilitation of enzymes to break covalent bonds. Water can be incorporated directly during hydrolysis (e.g. aldolase), or indirectly whilst the abstracted hydrogen resides on the enzyme residue (e.g. TPI and PGI). In the latter case, isotopic equilibrium is not guaranteed with a high degree of intramolecular transfer noted during unidirectional assessment of PGI (Rose & O'Connell, 1961; Noltman, 1972; Malaisse *et al.*, 1991) and TPI (especially in

the direction glyceraldehyde-3-phosphate to dihydroxyacetone phosphate; O'Donoghue *et al.*, 2005a,b). In other words, even if a reaction proceeds, hydrogen exchange with water is not systematic. Additionally, for hydrogen, there are also opportunities for large kinetic isotope effects (KIE) to occur that do not involve water (e.g. glucose-6-phosphate dehydrogenase, KIE = 2.97; Hermes & Cleland, 1984; glyceraldehyde-3-phosphate dehydrogenase, KIE = 1.89; Canellas & Cleland, 1991), which were not considered in the original interpretation of isotope effects associated with cellulose production in the Yakir & DeNiro model (1990).

Therefore, there are two important differences in the mechanisms shaping isotope variability between hydrogen and oxygen: (1) First,  $f_O$  and  $f_H$  are unlikely to covary given that isotopic exchange with water can occur spontaneously for oxygen (independent of C fluxes), and intramolecular transfer for hydrogen (with  $^1\text{H}/^2\text{H}$  isotope effects) may introduce variable isotope fractionations (dependent on carbon fluxes and metabolic pathways).

(2) Second,  $^{16}\text{O}/^{18}\text{O}$  isotope effects are mostly equilibrium isotope effects (dependent on temperature but otherwise considered constant; Sternberg & Ellsworth, 2011), whereas hydrogen metabolism involves additional kinetic isotope effects (observed isotope effect dependent on metabolite partitioning; Hayes, 2001).

Therefore, it is conceivable that oxygen and hydrogen could show different environmentally induced metabolic dependencies. These metabolic effects thus impact on key parameters describing cellulose isotope variability (Eqn 3):  $f_O$  and  $f_H$ , and fractionation factors,  $\epsilon$ . They are anticipated to depend on organs, since leaves and branches have contrasting carbohydrate metabolisms, as explained below.

### Metabolic differences at the origin of leaf-branch wood isotope patterns

As found here and elsewhere (e.g. Kahmen *et al.*, 2011; Cheesman & Cernusak, 2016), wood cellulose  $\delta^{18}\text{O}$  values tend to be lower than leaf cellulose  $\delta^{18}\text{O}$  values. A number of previously proposed mechanisms have rationalised the relative  $^{18}\text{O}$ -depletion of wood compared with leaf cellulose according to either (1) that 'metabolic' water in which sugars and cellulose are synthesised is  $^{18}\text{O}$ -depleted in heterotrophic tissues compared with leaves (Cernusak *et al.*, 2005; Gessler *et al.*, 2013; Cheesman & Cernusak, 2016; Zhu *et al.*, 2020); and/or, (2) that the extent of isotopic exchange in heterotrophic tissues is greater than that in leaf tissue (Cheesman & Cernusak, 2016). Indeed, when we eliminated the discrepancy between observed and modelled  $\delta^{18}\text{O}$  values by allowing  $f_O$  estimates to vary, our results indicated that  $f_O$  differed between tissues (estimates in branch wood > leaves; Fig. 6a) and was negatively related to mean annual precipitation (slope of  $f_O$  vs MAP for branch wood > leaves; Fig. 6a). Strikingly, the environmental sensitivity of  $f_O$  in branch wood cellulose with MAP was statistically the same as determined for branch wood cellulose of eucalypts across a similar aridity gradient in Queensland, Australia (Fig. 6b; Cheesman & Cernusak, 2016).

**Table 1** Isotopic measurements (‰) for oxygen ( $\delta^{18}\text{O}$ ) and hydrogen ( $\delta^2\text{H}$ ) of xylem water, cellulose and modelled seasonally integrated leaf water, averaged (with standard deviation) by site and for all species along the north Australian aridity gradient.

Location	Site code <sup>a</sup>	Observed xylem water <sup>b</sup>		Observed leaf cellulose		Observed wood cellulose		Seasonally integrated ave. modelled leaf water <sup>c</sup>	
		$\delta^{18}\text{O}$	$\delta^2\text{H}$	$\delta^{18}\text{O}$	$\delta^2\text{H}$	$\delta^{18}\text{O}$	$\delta^2\text{H}$	$\delta^{18}\text{O}$	$\delta^2\text{H}$
Darwin	<b>1</b>	-6.50 ± 0.45	-52.31 ± 2.25	36.96 ± 2.15	-9.68 ± 20.02	29.60 ± 2.05	4.43 ± 12.03	17.92 ± 0.46	14.53 ± 2.41
Adelaide River	<b>2</b>	-7.08 ± 0.36	-58.47 ± 4.73	37.40 ± 1.69	-26.25 ± 5.38	30.45 ± 0.96	-7.08 ± 8.86	17.66 ± 0.37	7.96 ± 5.07
Katherine	<b>3</b>	8.45 ± 0.74	-69.52 ± 4.52	37.58 ± 3.04	-31.99 ± 13.36	29.63 ± 1.25	-24.32 ± 9.55	16.52 ± 0.76	-3.19 ± 4.84
Larrimah	<b>4</b>	-7.76 ± 0.53	-66.78 ± 3.32	33.03 ± 3.23	-35.61 ± 10.46	29.70 ± 0.83	-23.88 ± 11.67	16.94 ± 0.54	-1.82 ± 3.55
Daly Waters	<b>5</b>	-7.67 ± 0.38	-64.25 ± 2.25	30.05 ± 2.67	-45.57 ± 5.86	28.42 ± 1.09	-37.30 ± 7.21	15.41 ± 0.39	-3.85 ± 2.40
Elliott	<b>6</b>	-7.39 ± 0.56	-64.14 ± 1.94	34.31 ± 3.43	-39.22 ± 10.16	28.54 ± 1.57	-28.68 ± 15.14	14.06 ± 0.57	-8.43 ± 2.06
Hellen Springs	<b>7</b>	-9.73 ± 0.33	-78.41 ± 1.42	34.66 ± 2.48	-43.16 ± 13.42	28.40 ± 0.78	-38.00 ± 6.23	10.68 ± 0.34	-25.93 ± 1.50
Tennant Creek	<b>8</b>	-7.89 ± 0.59	-70.18 ± 1.99	33.91 ± 3.27	-40.44 ± 10.33	27.90 ± 1.27	-33.56 ± 8.68	10.03 ± 0.60	-23.82 ± 2.09
Barrow Creek	<b>9</b>	-7.70 ± 0.16	-64.78 ± 1.59	32.87 ± 3.64	-21.55 ± 7.96	27.31 ± 1.78	-12.00 ± 9.07	8.65 ± 0.16	-21.56 ± 1.67
Territory Grape Farm	<b>10</b>	-6.27 ± 0.55	-48.66 ± 1.68	33.80 ± 1.31	-17.98 ± 10.58	30.02 ± 1.23	-4.21 ± 6.78	8.50 ± 0.56	-9.62 ± 1.75
Alice Springs	<b>11</b>	-6.72 ± 0.47	-52.87 ± 3.02	28.17 ± 1.00	-37.28 ± 8.33	28.01 ± 1.08	-23.69 ± 7.46	6.14 ± 0.47	-18.91 ± 3.13
Observed range <sup>d</sup> $\delta$		4.53	34.75	16.42	89.66	7.81	79.17		
Site range <sup>e</sup> $\Delta$				8.61	28.52	1.37	29.06	11.63	34.67

Samples are taken from dominant acacia and eucalypt tree species.

<sup>a</sup>Sites in bold correspond to the sites represented in Kahmen *et al.* (2013). Site coordinates are given in Supporting Information Dataset S1.

<sup>b</sup>Source: Cernusak *et al.* (2016) – data averaged from both the March/April and September sampling campaigns.

<sup>c</sup>Refer to Table S2 for model inputs. Variation is a result of sampled xylem water used as direct input and estimated water vapour  $\delta$ , which was assumed in equilibrium with xylem water. All other model inputs are site averaged.

<sup>d</sup>Calculated as maximum–minimum observed  $\delta$  values from individual data points (see Dataset S1 for individual data points).

<sup>e</sup> $\Delta$  calculated from site averages as  $(\delta_{\text{variable}} - \delta_{\text{xylem water}}) / (1 + \delta_{\text{xylem water}})$  and then the range computed as Site 1–Site 11 to reflect the expected gradient in leaf water enrichment values.

**Table 2** Parameter values for slope and intercepts of significant ( $P < 0.05$ ) correlations of  $\delta^2\text{H}$  vs  $\delta^{18}\text{O}$  for water and cellulose data presented in Fig. 2(a), fitted using standard major axis regression.

Sample	Slope	Intercept	$R^2$	$n$
Water vapour <sup>a</sup>	7.41	6.37	0.99	332
Xylem water <sup>a</sup>	9.17	7.94	0.83	132
Leaf water	2.93	-43.25	0.69	332
Leaf cellulose <sup>b</sup>	3.47	-148.58	0.17	132
Branch wood cellulose <sup>c</sup>	10.78	-332.99	0.08	132

<sup>a</sup>Slope significantly different from global meteoric water line of 8.

<sup>b</sup>Slope significantly different ( $P = 0.045$ ) from that of leaf water correlation but within 95% CI.

<sup>c</sup>Slope not significantly different from that of xylem water correlation.

In principle, mechanisms driving  $\delta^{18}\text{O}$  tissue patterns should also be applicable to hydrogen. In the first case (mechanism 1 above),  $^2\text{H}$ -depleted water in heterotrophic tissues should similarly result in  $^2\text{H}$ -depleted branch wood cellulose relative to leaf cellulose (all else being equal). In the second case (mechanism 2), greater isotopic exchange should result in the opposite pattern with  $^2\text{H}$ -enriched branch wood relative to leaf cellulose (due to the particularly large isotopic fractionations during heterotrophic metabolism as discussed in the Introduction section). There are only two studies that we could find that compared leaf/needle and wood cellulose  $\delta^2\text{H}$  values to assess the likelihood of either mechanism: in piñon pine (*Pinus edulis* and *Pinus monophylla*) sampled intra-annually, needle and stem wood  $\delta^2\text{H}$  values were similar (Pendall *et al.*, 2005); whereas in avocado (*Persea americana*) grown from seed in terrariums, there was a variable  $\delta^2\text{H}$  offset between tissues, even within a relative humidity treatment (Terwilliger & Deniro, 1995). Nonetheless, both studies concluded that whilst leaf cellulose  $\delta^2\text{H}$  values retained the leaf water climatic signal, the strength of the signal retention in stem cellulose varied. To this end, Terwilliger & Deniro (1995) hypothesised that the extent to which stem cellulose reflected leaf water isotope signals depended on internal metabolic drivers, which impact on postphotosynthetic processes, including the reliance on stored C vs current assimilates. Although direct evidence is still lacking, the idea that different internal C sources may have different  $\delta^2\text{H}$  values was also recently proposed by Lehmann *et al.* (2021) and may be another mechanism that differentiates O and H in terms of isotopic effects leading to weakened covariation.

In comparison with the other two studies, we found that branch wood cellulose was  $^2\text{H}$ -enriched compared with leaf cellulose; although, the offset was statistically nonsignificant according to the intercept of Fig. 3. The simplest interpretation of the consistency in  $\delta^2\text{H}$  values between organs is that hydrogen is less sensitive to isotopic exchange during sink cell metabolism. This may be the consequence of either intramolecular transfer and/or because equilibrium fractionation is smaller than the estimated value of 158‰, resulting in an insensitivity to isotopic exchange. Given the large kinetic isotope effects associated with dehydrogenase reactions (discussed in the 'Principle of biochemistry impacting on  $\delta^{18}\text{O}$  and  $\delta^2\text{H}$ ' in the Discussion section), it is

plausible that the value estimated for isotope fractionation during exchange with water in Yakir & DeNiro (1990) is a composite of equilibrium and kinetic isotope effects. Furthermore, it was recently shown that the majority of leaf cellulose  $\delta^2\text{H}$  variation across species could be explained by isotope fractionation during sucrose synthesis (Holloway-Phillips *et al.*, 2022), and at the position-specific level,  $^2\text{H}$ -enrichment in wood could be explained by isotope effects on carbon-bound positions H-1 and H-2 of glucose, which was assumed to originate from source leaves (Wieloch *et al.*, 2022b). Therefore, we hypothesise that the similarity in the  $\delta^2\text{H}$  values between organs may reflect biosynthetic variability induced during photosynthesis and before sucrose export ('source-cell isotope effects'). Consequently, we suggest that it is the different metabolic isotope signals captured by each element that led to a loss of covariation, particularly in branch wood material where isotopic exchange of oxygen with water appeared to be particularly responsive to metabolic-induced responses to aridity.

### Interpreting the metabolic isotope signals

The lack of environmental predictability to the hydrogen metabolic signal may reflect the shift in species identity across the aridity gradient, since species differences in cellulose  $\delta^2\text{H}$  values and biosynthetic isotope effects associated with source-cell metabolism have recently been noted (Holloway-Phillips *et al.*, 2022; Lehmann *et al.*, 2022; Baan *et al.*, 2023; Schuler *et al.*, 2023). Conversely, the trend towards increasing isotopic exchange of oxygen with water with increasing aridity may be supported by ecological knowledge of the sites, as suggested below.

Isotopic exchange has been experimentally linked to the cycling of triose-hexose phosphates (Hill *et al.*, 1995), which led to the suggestion by Barbour & Farquhar (2000) and experimentally supported by Song *et al.* (2014), that the longer the residence time of sugars within sink cells, the greater the opportunity for metabolite cycling and hence isotopic exchange. This cycle often interacts with a cycle of sucrose synthesis and degradation (Dancer *et al.*, 1990; Hatzfeld & Stitt, 1990). Altogether, these cycles are thought to allow for large and rapid changes in the net rate of sucrose breakdown in response to the demand in the cell (e.g. during stress events), whilst minimising changes in steady-state concentrations of metabolites (Geigenberger, 2003). In applying this interpretation to  $f_{\text{O}}$  changes, it would therefore suggest that metabolite cycling (and/or the flux through the cycle) increases with increasing aridity, particularly in heterotrophic tissues.

Despite significant periods of absent rain throughout the transient and decreasing predictability of rainfall patterns (Rogers & Beringer, 2017), plant water stress of the woody overstorey is minimal based on measures of leaf water potential, water use (O'Grady *et al.*, 1999; Eamus *et al.*, 2000; Hutley *et al.*, 2001) and  $\delta^{13}\text{C}$  (Schulze *et al.*, 1998; Miller *et al.*, 2001). Furthermore, modelling suggests shifts in growth strategies and C allocation to capitalise on small, isolated rain events (Cook & Heerdegen, 2001; Cook *et al.*, 2002). As such, the capacity to respond opportunistically to rainfall may be facilitated by



increased metabolite cycling. To test this hypothesis, it would be interesting to use the approach of Hill *et al.* (1995) to determine whether there are shifts in metabolite cycling along the transect, aligned with shifts in  $f_O$  estimates. Similarly, to investigate the relative importance of intramolecular hydrogen transfer during cytosolic metabolism as the reason for why shifts in  $f_O$  and  $f_H$  may not covary, analysing the position-specific  $\delta^2H$  of glucosyl and fructosyl moieties of sucrose may be useful, particularly when combined with  $^{13}C$  labelling to quantify flux changes and cycling rates (e.g. Krook *et al.*, 2000; van der Merwe *et al.*, 2010).

### Limitations and implications

Whilst  $\delta^{18}O$  has generally been found to retain climatic signals in tree-ring series, we did not observe that here. In fact, the cellulose isotope model predicted the observed isotopic variability better for  $\delta^2H$  in wood ( $R^2 = 0.35$ ; Fig. 4). This perhaps reflects the larger range in isotopic variability associated with plant water pools in hydrogen compared with oxygen, relative to that induced by metabolism (inferred from the range in expected values vs the scatter around the line in Fig. 4). Thus, our data have demonstrated that metabolic-induced isotopic variation is not only an issue that needs to be considered for hydrogen, but also for oxygen, especially over large spatial gradients where plant adaptation has occurred. In this regard, due to confounding changes in environmental parameters across sites and species shifts, the transfer of climatic isotope signals from plant water pools to leaf and wood cellulose should be isolated and experimentally tested before space-for-time experimental results are applied to understand temporal variation in isotopic data (e.g. to tree-ring time series). This similarly applies to understanding (and thus modelling) the drivers of metabolic-induced isotope variability. Specifically, the link between aridity and isotopic exchange with water needs to be independently tested within a given species, where all other environmental factors remain the same.

In addition, model inversion to estimate model parameters from cellulose  $\delta$  values is only as good as the input data, as was recently highlighted by Lin *et al.* (2022). In the current study, this meant modelling leaf water  $\delta$  values. Whilst the leaf water model successfully predicted diurnally measured  $\delta$  values (Kahmen *et al.*, 2013), a number of simplifying assumptions were made to provide seasonal averages applicable to the time integration of cellulose synthesis (Table S2). Determining the relevant climate period captured within the sugar used for cellulose synthesis depends on the synchrony of assimilation and growth and sugar pool mixing processes including the use of previously stored C. Determining this period remains a major challenge for the field, but progress is being made with the development of process-based modelling solutions (e.g. Hirl *et al.*, 2021).

Critically, our data have demonstrated that the metabolic information captured by each element and plant tissue differs. Whilst this drives the decoupling between  $\delta^{18}O$  and  $\delta^2H$  and therefore complicates efforts to combine isotopic information for estimating climatic parameters (e.g. Voelker *et al.*, 2014), it

points to new opportunities to explore different aspects of plant metabolic responses to the environment.

### Acknowledgements

We thank Stefan Arndt at University of Melbourne, Australia, for his assistance in the organisation and sample collection during the original field campaign, and Svenja Förster at the University of Basel, Switzerland, for assistance with the cellulose and lipid extractions. This project was made possible by funding from the European Research Council (ERC) under the European Union's Horizon 2020 research and innovation programme (grant agreement no. 724750). This grant employed MH-P, with additional funding assistance by the Swiss National Science Foundation (no. 205492) during the revision and publication stages of this manuscript. MML was funded by the SNF Ambizione grant (no. 179978). GT was funded by the *Région Pays de la Loire* via the Connect Talent grant (Ioseed). Open access funding provided by Universitat Basel.







### Competing interests

None declared.

### Author contributions

MH-P, AK and LAC conceived the study. MH-P conducted and analysed the isotopic data. MML and DBN provided lab assistance. MH-P interpreted the results with feedback and input from all authors. MH-P developed the isotopic hypotheses in consultation with GT. MH-P wrote the paper with contributions from all authors.

### ORCID

Lucas A. Cernusak  <https://orcid.org/0000-0002-7575-5526>  
Meisha Holloway-Phillips  <https://orcid.org/0000-0002-8353-3536>  
Ansgar Kahmen  <https://orcid.org/0000-0002-7823-5163>  
Marco M. Lehmann  <https://orcid.org/0000-0003-2962-3351>  
Daniel B. Nelson  <https://orcid.org/0000-0002-2716-7770>  
Guillaume Tcherkez  <https://orcid.org/0000-0002-3339-956X>

### Data availability

Measured isotope values and site information used in the analyses presented in this paper are available in Dataset S1. Equations required to estimate modelled cellulose isotope values and derived parameters (e.g.  $f_O$ ) are given in Table S2.

### References

- An W, Liu X, Leavitt SW, Xu G, Zeng X, Wang W, Qin D, Ren J. 2014. Relative humidity history on the Batang–Litang Plateau of western China since 1755 reconstructed from tree-ring  $\delta^{18}O$  and  $\delta D$ . *Climate Dynamics* 42: 2639–2654.

- Augusti A, Betson TR, Schleucher J. 2006. Hydrogen exchange during cellulose synthesis distinguishes climatic and biochemical isotope fractionations in tree rings. *New Phytologist* 172: 490–499.
- Baan J, Holloway-Phillips M, Nelson DB, Kahmen A. 2022. The metabolic sensitivity of hydrogen isotope fractionation differs between plant compounds. *Phytochemistry* 207: 113563.
- Baan J, Holloway-Phillips M, Nelson DB, Kahmen A. 2023. Species and biosynthetic effects cause uncorrelated variation in oxygen and hydrogen isotope compositions of plant organic compounds. *Geochimica et Cosmochimica Acta* 352: 1–13.
- Barbour MM, Farquhar GD. 2000. Relative humidity- and ABA-induced variation in carbon and oxygen isotope ratios of cotton leaves. *Plant, Cell & Environment* 23: 473–485.
- Barnard R, Salmon Y, Kodama N, Sörgel K, Holst J, Rennenberg H, Gessler A, Buchmann N. 2007. Evaporative enrichment and time lags between  $\delta^{18}\text{O}$  of leaf water and organic pools in a pine stand. *Plant, Cell & Environment* 30: 539–550.
- Bivand R, Keitt T, Rowlingson B. 2023. *rgdal: bindings for the 'Geospatial' data abstraction library*. [WWW document] URL <https://CRAN.R-project.org/package=rgdal> [accessed 22 May 2023].
- Boettger T, Haupt M, Friedrich M, Waterhouse JS. 2014. Reduced climate sensitivity of carbon, oxygen and hydrogen stable isotope ratios in tree-ring cellulose of silver fir (*Abies alba* Mill.) influenced by background  $\text{SO}_2$  in Franconia (Germany, Central Europe). *Environmental Pollution* 185: 281–294.
- Canellas PF, Cleland WW. 1991. Carbon-13 and deuterium isotope effects on the reaction catalyzed by glyceraldehyde-3-phosphate dehydrogenase. *Biochemistry* 30: 8871–8876.
- Cernusak L, Farquhar G, Pate J. 2005. Environmental and physiological controls over oxygen and carbon isotope composition of Tasmanian blue gum, *Eucalyptus globulus*. *Tree Physiology* 25: 129–146.
- Cernusak LA, Barbata A, Bush RT, Eichstaedt R, Ferrio JP, Flanagan LB, Gessler A, Martín-Gómez P, Hirl RT, Kahmen A *et al.* 2022. Do  $^2\text{H}$  and  $^{18}\text{O}$  in leaf water reflect environmental drivers differently? *New Phytologist* 235: 41–51.
- Cernusak LA, Barbour MM, Arndt SK, Cheesman AW, English NB, Feild TS, Helliiker BR, Holloway-Phillips MM, Holtum JAM, Kahmen A *et al.* 2016. Stable isotopes in leaf water of terrestrial plants. *Plant, Cell & Environment* 39: 1087–1102.
- Cernusak LA, Wong S-C, Farquhar GD. 2003. Oxygen isotope composition of phloem sap in relation to leaf water in *Ricinus communis*. *Functional Plant Biology* 30: 1059–1070.
- Cheesman AW, Cernusak LA. 2016. Infidelity in the outback: climate signal recorded in  $\Delta^{18}\text{O}$  of leaf but not branch cellulose of eucalypts across an Australian aridity gradient. *Tree Physiology* 37: 554–564.
- Cook GD, Heerdegen RG. 2001. Spatial variation in the duration of the rainy season in monsoonal Australia. *International Journal of Climatology* 21: 1723–1732.
- Cook GD, Williams RJ, Hutley LB, O'Grady AP, Liedloff AC. 2002. Variation in vegetative water use in the savannas of the North Australian Tropical Transect. *Journal of Vegetation Science* 13: 413–418.
- Cormier MA, Werner RA, Leuenberger MC, Kahmen A. 2019.  $^2\text{H}$ -enrichment of cellulose and n-alkanes in heterotrophic plants. *Oecologia* 189: 365–373.
- Cormier M-A, Werner RA, Sauer PE, Gröcke DR, Leuenberger MC, Wieloch T, Schleucher J, Kahmen A. 2018.  $^2\text{H}$ -fractionations during the biosynthesis of carbohydrates and lipids imprint a metabolic signal on the  $\delta^2\text{H}$  values of plant organic compounds. *New Phytologist* 218: 479–491.
- Dancer J, Hatzfeld W-D, Stitt M. 1990. Cytosolic cycles regulate the turnover of sucrose in heterotrophic cell-suspension cultures of *Chenopodium rubrum* L. *Planta* 182: 223–231.
- DeNiro MJ, Epstein S. 1981. Isotopic composition of cellulose from aquatic organisms. *Geochimica et Cosmochimica Acta* 45: 1885–1894.
- Dongmann G, Nürnberg HW, Förstel H, Wagener K. 1974. On the enrichment of  $\text{H}_2^{18}\text{O}$  in the leaves of transpiring plants. *Radiation and Environmental Biophysics* 11: 41–52.
- Eamus D, O'Grady AP, Hutley L. 2000. Dry season conditions determine wet season water use in the wet-tropical savannas of northern Australia. *Tree Physiology* 20: 1219–1226.
- Epstein S, Yapp CJ, Hall JH. 1976. The determination of the D/H ratio of non-exchangeable hydrogen in cellulose extracted from aquatic and land plants. *Earth and Planetary Science Letters* 30: 241–251.
- Farquhar GD, Barbour MM, Henry BK. 1998. Interpretation of oxygen isotope composition of leaf material. In: Griffiths H, ed. *Stable isotopes: integration of biological, ecological, and geochemical processes*. Oxford, UK: BIOS Scientific, 27–48.
- Farquhar GD, Lloyd J. 1993. Carbon and oxygen isotope effects in the exchange of carbon dioxide between terrestrial plants and the atmosphere. In: Ehleringer JR, Hall AE, Farquhar GD, eds. *Stable isotopes and plant carbon-water relations*. San Diego, CA, USA: Academic Press, 47–70.
- Flanagan LB, Comstock JP, Ehleringer JR. 1991. Comparison of modeled and observed environmental influences on the stable oxygen and hydrogen isotope composition of leaf water in *Phaseolus vulgaris* L. *Plant Physiology* 96: 588–596.
- Garnier S, Ross N, Rudis R, Camarago A, Sciaini M, Scherer C. 2022. *RVISION – colorblind-friendly color maps for R*. [WWW document] URL <https://sjmgarnier.github.io/iridis/> [accessed 22 May 2023].
- Gaudinski JB, Dawson TE, Quideau S, Schuur EA, Roden JS, Trumbore SE, Sandquist DR, Oh SW, Wasylishen RE. 2005. Comparative analysis of cellulose preparation techniques for use with  $^{13}\text{C}$ ,  $^{14}\text{C}$ , and  $^{18}\text{O}$  isotopic measurements. *Analytical Chemistry* 77: 7212–7224.
- Geigenberger P. 2003. Response of plant metabolism to too little oxygen. *Current Opinion in Plant Biology* 6: 247–256.
- Gessler A, Brandes E, Keitel C, Boda S, Kayler ZE, Granier A, Barbour M, Farquhar GD, Treydte K. 2013. The oxygen isotope enrichment of leaf-exported assimilates – does it always reflect lamina leaf water enrichment? *New Phytologist* 200: 144–157.
- Gessler A, Ferrio JP, Hommel R, Treydte K, Werner RA, Monson RK. 2014. Stable isotopes in tree rings: towards a mechanistic understanding of isotope fractionation and mixing processes from the leaves to the wood. *Tree Physiology* 34: 796–818.
- Gori Y, Wehrens R, La Porta N, Camin F. 2015. Oxygen and hydrogen stable isotope ratios of bulk needles reveal the geographic origin of Norway spruce in the European Alps. *PLoS ONE* 10: e0118941.
- Gray J, Thompson P. 1976. Climatic information from  $^{18}\text{O}/^{16}\text{O}$  ratios of cellulose in tree rings. *Nature* 262: 481–482.
- Hafner P, Robertson I, McCarrroll D, Loader NJ, Gagen M, Bale RJ, Jungner H, Sonninen E, Hilasvuori E, Levanič T. 2011. Climate signals in the ring widths and stable carbon, hydrogen and oxygen isotopic composition of *Larix decidua* growing at the forest limit in the southeastern European Alps. *Trees* 25: 1141–1154.
- Hatzfeld W-D, Stitt M. 1990. A study of the rate of recycling of triose phosphates in heterotrophic *Chenopodium rubrum* cells, potato tubers, and maize endosperm. *Planta* 180: 198–204.
- Hayes JM. 2001. Fractionation of carbon and hydrogen isotopes in biosynthetic processes. In: Valley JW, Cole DR, eds. *Stable isotope geochemistry*. Berlin, Germany: De Gruyter, 225–278.
- Helliiker BR, Richter SL. 2008. Subtropical to boreal convergence of tree-leaf temperatures. *Nature* 454: 511–514.
- Hermes JD, Cleland WW. 1984. Evidence from multiple isotope effect determinations for coupled hydrogen motion and tunneling in the reaction catalyzed by glucose-6-phosphate dehydrogenase. *Journal of the American Chemical Society* 106: 7263–7264.
- Hijmans R. 2023. *RASTER: geographic data analysis and modeling*. [WWW document] URL <https://CRAN.R-project.org/package=raster> [accessed 22 May 2023].
- Hill SA, Waterhouse JS, Field EM, Switsur VR, Ap Rees T. 1995. Rapid recycling of triose phosphates in oak stem tissue. *Plant, Cell & Environment* 18: 931–936.
- Hirl RT, Ogée J, Ostler U, Schäufele R, Baca Cabrera JC, Zhu J, Schleip I, Wingate L, Schnyder H. 2021. Temperature-sensitive biochemical  $^{18}\text{O}$ -fractionation and humidity-dependent attenuation factor are needed to predict  $\delta^{18}\text{O}$  of cellulose from leaf water in a grassland ecosystem. *New Phytologist* 229: 3156–3171.
- Holloway-Phillips M, Baan J, Nelson DB, Lehmann MM, Tcherkez G, Kahmen A. 2022. Species variation in the hydrogen isotope composition of

- leaf cellulose is mostly driven by isotopic variation in leaf sucrose. *Plant, Cell & Environment* 45: 2636–2651.
- Hutchinson M, Tingbao X, Kesteven J. 2014. *Monthly 1976–2005 mean precipitation: ANUclimate 1.0, 0.01 degree, Australian coverage*. Canberra, ACT, Australia: Australian National University. [WWW document] URL <https://portal.tern.org.au/metadata/NCI/6617f064-1ed9-4548-a06a-cc91feae280> [accessed 22 May 2023].
- Hutley LB, Beringer J, Isaac PR, Hacker JM, Cernusak LA. 2011. A sub-continental scale living laboratory: spatial patterns of savanna vegetation over a rainfall gradient in northern Australia. *Agricultural and Forest Meteorology* 151: 1417–1428.
- Hutley LB, O'Grady AP, Eamus D. 2001. Monsoonal influences on evapotranspiration of savanna vegetation of northern Australia. *Oecologia* 126: 434–443.
- Hvitfeldt E. 2022. *PRISMATIC: color manipulation tools*. [WWW document] URL <https://CRAN.R-project.org/package=prismatic> [accessed 22 May 2023].
- Ish-Shalom-Gordon N, Lin G, Da Silveira Lobo Sternberg L. 1992. Isotopic fractionation during cellulose synthesis in two mangrove species: salinity effects. *Phytochemistry* 31: 2623–2626.
- Kahmen A, Hoffmann B, Schefuß E, Arndt SK, Cernusak LA, West JB, Sachse D. 2013. Leaf water deuterium enrichment shapes leaf wax n-alkane  $\delta D$  values of angiosperm plants II: observational evidence and global implications. *Geochimica et Cosmochimica Acta* 111: 50–63.
- Kahmen A, Sachse D, Arndt SK, Tu KP, Farrington H, Vitousek PM, Dawson TE. 2011. Cellulose  $\delta^{18}O$  is an index of leaf-to-air vapor pressure difference (VPD) in tropical plants. *Proceedings of the National Academy of Sciences, USA* 108: 1981–1986.
- Kimak A, Kern Z, Leuenberger M. 2015. Qualitative distinction of autotrophic and heterotrophic processes at the leaf level by means of triple stable isotope (C-O-H) patterns. *Frontiers in Plant Science* 6: 1008.
- Krook J, Vreugdenhil D, Dijkema C, Van Der Plas LHW. 2000. Uptake of  $^{13}C$ -glucose by cell suspensions of carrot (*Daucus carota*) measured by *in vivo* NMR: cycling of triose-, pentose- and hexose-phosphates. *Physiologia Plantarum* 108: 125–133.
- Leaney FW, Osmond CB, Allison GB, Ziegler H. 1985. Hydrogen-isotope composition of leaf water in  $C_3$  and  $C_4$  plants: its relationship to the hydrogen-isotope composition of dry matter. *Planta* 164: 215–220.
- Lehmann MM, Schuler P, Cormier M-A, Allen ST, Leuenberger M, Voelker S. 2022. The stable hydrogen isotopic signature: from source water to tree rings. In: Siegwolf RTW, Brooks JR, Roden J, Saurer M, eds. *Stable isotopes in tree rings: inferring physiological, climatic and environmental responses*. Cham, Switzerland: Springer International, 331–359.
- Lehmann MM, Vitali V, Schuler P, Leuenberger M, Saurer M. 2021. More than climate: hydrogen isotope ratios in tree rings as novel plant physiological indicator for stress conditions. *Dendrochronologia* 65: 125788.
- Libby LM, Pandolfi LJ, Payton PH, Marshall J, Becker B, Giertz-Sienbenlist V. 1976. Isotopic tree thermometers. *Nature* 261: 284–288.
- Lin W, Barbour MM, Song X. 2022. Do changes in tree-ring  $\delta^{18}O$  indicate changes in stomatal conductance? *New Phytologist* 236: 803–808.
- Liu HT, Schäufele R, Gong XY, Schnyder H. 2017. The  $\delta^{18}O$  and  $\delta^2H$  of water in the leaf growth-and-differentiation zone of grasses is close to source water in both humid and dry atmospheres. *New Phytologist* 214: 1423–1431.
- Loader NJ, Santillo PM, Woodman-Ralph JP, Rolfe JE, Hall MA, Gagen M, Robertson I, Wilson R, Froyd CA, McCarroll D. 2008. Multiple stable isotopes from oak trees in southwestern Scotland and the potential for stable isotope dendroclimatology in maritime climatic regions. *Chemical Geology* 252: 62–71.
- Malaisse WJ, Liemans V, Malaisse-Lagae F, Ottinger R, Willem R. 1991. Phosphoglucosomerase-catalyzed interconversion of hexose phosphates. *Molecular and Cellular Biochemistry* 103: 131–140.
- McCarroll D, Loader NJ. 2004. Stable isotopes in tree rings. *Quaternary Science Reviews* 23: 771–801.
- McInerney FA, Gerber C, Dangerfield E, Cernusak LA, Puccini A, Szarvas S, Singh T, Welti N. 2023. Leaf water  $\delta^{18}O$ ,  $\delta^2H$  and  $d$ -excess isoscapes for Australia using region-specific plant parameters and non-equilibrium vapour. *Hydrological Processes* 37: e14878.
- Meier-Augenstein W, Kemp HF, Schenk ER, Almirall JR. 2014. Discrimination of unprocessed cotton on the basis of geographic origin using multi-element stable isotope signatures. *Rapid Communications in Mass Spectrometry* 28: 545–552.
- van der Merwe MJ, Groenewald JH, Stitt M, Kossmann J, Botha FC. 2010. Downregulation of pyrophosphate: D-fructose-6-phosphate 1-phosphotransferase activity in sugarcane culms enhances sucrose accumulation due to elevated hexose-phosphate levels. *Planta* 231: 595–608.
- Miller JM, Williams RJ, Farquhar GD. 2001. Carbon isotope discrimination by a sequence of *Eucalyptus* species along a subcontinental rainfall gradient in Australia. *Functional Ecology* 15: 222–232.
- Nabeshima E, Nakatsuka T, Kagawa A, Hiura T, Funada R. 2018. Seasonal changes of  $\delta D$  and  $\delta^{18}O$  in tree-ring cellulose of *Quercus crispula* suggest a change in post-photosynthetic processes during earlywood growth. *Tree Physiology* 38: 1829–1840.
- Nakatsuka T, Sano M, Li Z, Xu C, Tsushima A, Shigeoka Y, Sho K, Ohnishi K, Sakamoto M, Ozaki H *et al.* 2020. A 2600-year summer climate reconstruction in central Japan by integrating tree-ring stable oxygen and hydrogen isotopes. *Climate of the Past* 16: 2153–2172.
- Neuwirth E. 2022. *RCOLORBREWER: ColorBrewer palettes*. [WWW document] URL <https://CRAN.R-project.org/package=RColorBrewer> [accessed 22 May 2023].
- Nijzink RC, Schymanski SJ. 2022. Vegetation optimality explains the convergence of catchments on the Budyko curve. *Hydrology and Earth System Sciences* 26: 6289–6309.
- Noltman EA. 1972. Aldose-ketose isomerases. In: Boyer PD, ed. *The enzymes*. San Diego, CA, USA: Academic Press, 271–354.
- O'Donoghue AC, Amyes TL, Richard JP. 2005a. Hydron transfer catalyzed by triosephosphate isomerase. Products of isomerization of (r)-glyceraldehyde 3-phosphate in  $D_2O$ . *Biochemistry* 44: 2610–2621.
- O'Donoghue AC, Amyes TL, Richard JP. 2005b. Hydron transfer catalyzed by triosephosphate isomerase. Products of isomerization of dihydroxyacetone phosphate in  $D_2O$ . *Biochemistry* 44: 2622–2631.
- Offermann C, Ferrio JP, Holst J, Grote R, Siegwolf R, Kayler Z, Gessler A. 2011. The long way down – are carbon and oxygen isotope signals in the tree ring uncoupled from canopy physiological processes? *Tree Physiology* 31: 1088–1102.
- O'Grady AP, Eamus D, Hutley LB. 1999. Transpiration increases during the dry season: patterns of tree water use in eucalypt open-forests of northern Australia. *Tree Physiology* 19: 591–597.
- Pendall E, Williams DG, Leavitt SW. 2005. Comparison of measured and modeled variations in piñon pine leaf water isotopic enrichment across a summer moisture gradient. *Oecologia* 145: 605–618.
- Pierce D. 2023. *ncdf4: interface to Unidata netCDF (v.4 or earlier) format data files*. [WWW document] URL <https://CRAN.R-project.org/package=ncdf4> [accessed 22 May 2023].
- R Core Team. 2019. *R: a language and environment for statistical computing*. Vienna, Austria: R Foundation for Statistical Computing.
- Roden JS, Lin G, Ehleringer JR. 2000. A mechanistic model for interpretation of hydrogen and oxygen isotope ratios in tree-ring cellulose. *Geochimica et Cosmochimica Acta* 64: 21–35.
- Rogers CDW, Beringer J. 2017. Describing rainfall in northern Australia using multiple climate indices. *Biogeosciences* 14: 597–615.
- Rose IA, O'Connell EL. 1961. Intramolecular hydrogen transfer in the phosphoglucose isomerase reaction. *The Journal of Biological Chemistry* 236: 3086–3092.
- Ruppenthal M, Oelmann Y, del Valle HF, Wilcke W. 2015. Stable isotope ratios of nonexchangeable hydrogen in organic matter of soils and plants along a 2100-km climosequence in Argentina: new insights into soil organic matter sources and transformations? *Geochimica et Cosmochimica Acta* 152: 54–71.
- Sanchez-Bragado R, Serret MD, Marimon RM, Bort J, Araus JL. 2019. The hydrogen isotope composition  $\delta^2H$  reflects plant performance. *Plant Physiology* 180: 793–812.
- Schiegl WE, Vogel JC. 1970. Deuterium content of organic matter. *Earth and Planetary Science Letters* 7: 307–313.
- Schleucher J, Vanderveer P, Markley JL, Sharkey TD. 1999. Intramolecular deuterium distributions reveal disequilibrium of chloroplast phosphoglucose isomerase. *Plant, Cell & Environment* 22: 525–533.



- Schuler P, Cormier M-A, Werner RA, Buchmann N, Gessler A, Vitali V, Saurer M, Lehmann MM. 2022. A high-temperature water vapor equilibration method to determine non-exchangeable hydrogen isotope ratios of sugar, starch and cellulose. *Plant, Cell & Environment* 45: 12–22.
- Schuler P, Vitali V, Saurer M, Gessler A, Buchmann N, Lehmann MM. 2023. Hydrogen isotope fractionation in carbohydrates of leaves and xylem tissues follows distinct phylogenetic patterns: a common garden experiment with 73 tree and shrub species. *New Phytologist* 239: 547–561.
- Schulze ED, Williams RJ, Farquhar GD, Schulze W, Langridge J, Miller JM, Walker BH. 1998. Carbon and nitrogen isotope discrimination and nitrogen nutrition of trees along a rainfall gradient in northern Australia. *Functional Plant Biology* 25: 413–425.
- Song X, Barbour MM, Saurer M, Helliker BR. 2011. Examining the large-scale convergence of photosynthesis-weighted tree leaf temperatures through stable oxygen isotope analysis of multiple data sets. *New Phytologist* 192: 912–924.
- Song X, Farquhar GD, Gessler A, Barbour MM. 2014. Turnover time of the non-structural carbohydrate pool influences  $\delta^{18}\text{O}$  of leaf cellulose. *Plant, Cell & Environment* 37: 2500–2507.
- Song X, Lorrey A, Barbour MM. 2022. Environmental, physiological and biochemical processes determining the oxygen isotope ratio of tree-ring cellulose. In: Siegwolf RTW, Brooks JR, Roden J, Saurer M, eds. *Stable isotopes in tree rings: inferring physiological, climatic and environmental responses*. Cham, Switzerland: Springer International, 311–329.
- Sternberg L, Deniro MJ. 1983. Isotopic composition of cellulose from  $\text{C}_3$ ,  $\text{C}_4$ , and CAM plants growing near one another. *Science* 220: 947–949.
- Sternberg L, Ellsworth PFV. 2011. Divergent biochemical fractionation, not convergent temperature, explains cellulose oxygen isotope enrichment across latitudes. *PLoS ONE* 6: e28040.
- Terwilliger VJ, Deniro MJ. 1995. Hydrogen isotope fractionation in wood-producing avocado seedlings: biological constraints to paleoclimatic interpretations of  $\delta\text{D}$  values in tree ring cellulose nitrate. *Geochimica et Cosmochimica Acta* 59: 5199–5207.
- Vitali V, Martínez-Sancho E, Treydte K, Andreu-Hayles L, Dorado-Liñán I, Gutierrez E, Helle G, Leuenberger M, Loader NJ, Rinne-Garmston KT *et al.* 2022. The unknown third – hydrogen isotopes in tree-ring cellulose across Europe. *Science of the Total Environment* 813: 152281.
- Voelker SL, Brooks JR, Meinzer FC, Roden J, Pazdur A, Pawelczyk S, Hartsough P, Snyder K, Plavcová L, Šantrůček J. 2014. Reconstructing relative humidity from plant  $\delta^{18}\text{O}$  and  $\delta\text{D}$  as deuterium deviations from the global meteoric water line. *Ecological Applications* 24: 960–975.
- Warton DI, Duursma RA, Falster DS, Taskinen S. 2012. SMATR 3 – an R package for estimation and inference about allometric lines. *Methods in Ecology and Evolution* 3: 257–259.
- Wassenaar LI, Hobson KA, Sisti L. 2015. An online temperature-controlled vacuum-equilibration preparation system for the measurement of  $\delta^2\text{H}$  values of non-exchangeable-H and of  $\delta^{18}\text{O}$  values in organic materials by isotope-ratio mass spectrometry. *Rapid Communications in Mass Spectrometry* 29: 397–407.
- Waterhouse JS, Cheng S, Juchelka D, Loader NJ, McCarroll D, Switsur VR, Gautam L. 2013. Position-specific measurement of oxygen isotope ratios in cellulose: isotopic exchange during heterotrophic cellulose synthesis. *Geochimica et Cosmochimica Acta* 112: 178–191.
- Wickham H. 2016. *GGPLOT2: elegant graphics for data analysis*. New York, NY, USA: Springer-Verlag.
- Wieloch T, Augusti A, Schleucher J. 2022a. Anaplerotic flux into the Calvin–Benson cycle: hydrogen isotope evidence for *in vivo* occurrence in  $\text{C}_3$  metabolism. *New Phytologist* 234: 405–411.
- Wieloch T, Grabner M, Augusti A, Serk H, Ehlers I, Yu J, Schleucher J. 2022b. Metabolism is a major driver of hydrogen isotope fractionation recorded in tree-ring glucose of *Pinus nigra*. *New Phytologist* 234: 449–461.
- Yakir D. 1992. Variations in the natural abundance of oxygen-18 and deuterium in plant carbohydrates. *Plant, Cell & Environment* 15: 1005–1020.
- Yakir D, DeNiro MJ. 1990. Oxygen and hydrogen isotope fractionation during cellulose metabolism in *Lemma gibba* L. *Plant Physiology* 93: 325–332.
- Zhou Y, Zhang B, Stuart-Williams H, Grice K, Hocart CH, Gessler A, Kayler ZE, Farquhar GD. 2018. On the contributions of photorespiration and compartmentation to the contrasting intramolecular  $^2\text{H}$  profiles of  $\text{C}_3$  and  $\text{C}_4$  plant sugars. *Phytochemistry* 145: 197–206.
- Zhu Z, Yin X, Song X, Wang B, Ma R, Zhao Y, Rani A, Wang Y, Yan Q, Jing S *et al.* 2020. Leaf transition from heterotrophy to autotrophy is recorded in the intraleaf C, H and O isotope patterns of leaf organic matter. *Rapid Communications in Mass Spectrometry* 34: e8840.

## Supporting Information

Additional Supporting Information may be found online in the Supporting Information section at the end of the article.

**Dataset S1** Metadata and isotopic data used within this study.

**Fig. S1** Comparison of  $\delta^2\text{H}$  values between analytical methods for a subset of cellulose samples.

**Fig. S2** Relationship between observed and estimated leaf water delta values.

**Fig. S3** Fractional difference between predicted evaporative site isotopic enrichments.

**Fig. S4**  $f_{\text{O}}$  estimated with different model assumptions.

**Fig. S5** Simplified schematic of key reactions with isotope effects.

**Notes S1** Description and results of the sensitivity analysis.

**Table S1** Data sources for  $f_{\text{O}}$  and  $f_{\text{H}}$ .

**Table S2** Data inputs and model parameterisation of the cellulose isotope model.

**Table S3** Sensitivity analyses performed on cellulose isotope model parameters.

**Table S4** Coefficients from the regression of expected vs observed cellulose isotope values.

**Table S5** Slope values of the regression between  $\epsilon_{\text{exp-obs}}$  and MAP.

**Table S6** Coefficients of the regression between  $f_{\text{O}}$  and MAP for branch wood cellulose.

**Table S7** Summary of site averaged  $p_{\text{ex}}$ ,  $f_{\text{H}}$  and  $p_{\text{x}}$  estimates.

Please note: Wiley is not responsible for the content or functionality of any Supporting Information supplied by the authors. Any queries (other than missing material) should be directed to the *New Phytologist* Central Office.